An integrative assessment of the plastic debris load in the Mediterranean Sea

M.L. Pedrotti, Fabien Lombard, Alberto Baudena, François Galgani, Amanda Elineau, Stephanie Petit, Maryvonne Henry, Romain Troublé, Gilles Reverdin, Enrico Ser-Giacomi, et al.

Science of the Total Environment 838 (2022) 155958

Contents lists available at ScienceDirect

Science of the Total Environment

journal homepage: www.elsevier.com/locate/scitotenv

An integrative assessment of the plastic debris load in the Mediterranean Sea

Maria Luiza Pedrotti [a,*], Fabien Lombard [a,1], Alberto Baudena [a,1], François Galgani [b], Amanda Elineau [a], Stephanie Petit [a], Maryvonne Henry [c], Romain Troublé [d], Gilles Reverdin [e], Enrico Ser-Giacomi [f], Mikaël Kedzierski [g], Emmanuel Boss [h], Gabriel Gorsky [a]

[a] Sorbonne Universités, UPMC Université Paris 06, CNRS UMR 7093, LOV, Villefranche sur Mer, France
[b] IFREMER, Laboratoire LER/PAC, ZI Furiani, 20600 Bastia, France
[c] IFREMER, Laboratoire LER/PAC, La Seyne-sur-Mer, France
[d] The Tara Ocean Foundation, Paris, France
[e] Sorbonne Université CNRS/IRD/MNHN (LOCEAN/IPSL UMR 7159), Paris, France
[f] Dept. of Earth, Atmospheric and Planetary Sciences, Massachusetts Institute of Technology (MIT) Cambridge, MA, United States
[g] Université Bretagne Sud, UMR CNRS 6027, IRDL, F-56100 Lorient, France
[h] School of Marine Sciences, University of Maine, Orono, ME, United States

HIGHLIGHTS

- Plastics were analyzed using a ZoosCan in surface samples from Gibraltar to Lebanon
- An average of 2.60 × 10^5 plastic items km^{-2} was found in the Mediterranean Sea
- About 650 billion plastic weighing 660 tons float on the surface of the sea
- The lowest concentrations of plastic are found in the Levantine basin
- Advanced state of plastic degradation was observed in Mediterranean Sea

GRAPHICAL ABSTRACT

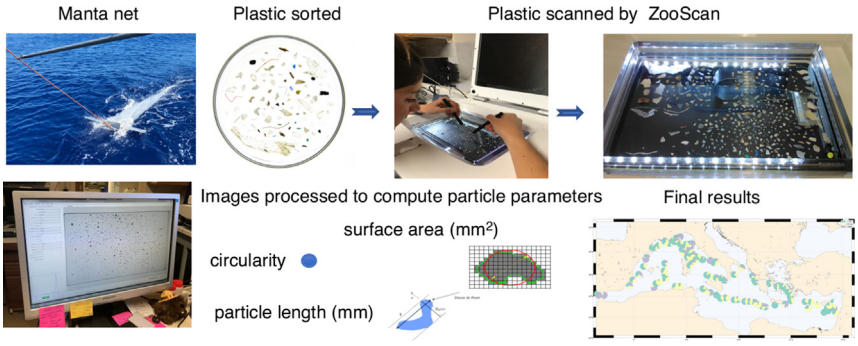

ARTICLE INFO

Editor: Damià Barceló

Keywords:
Plastic debris
Microplastic
TARA Mediterranean expedition
ZooScan
Mediterranean Sea
Sea surface

ABSTRACT

The Mediterranean Sea is recognized as one of the most polluted areas by floating plastics. During the Tara Mediterranean expedition, an extensive sampling of plastic debris was conducted in seven ecoregions, from Gibraltar to Lebanon with the aim of providing reliable estimates of regional differences in floating plastic loads and plastic characteristics. The abundance, size, surface, circularity and mass of 75,030 pieces were analyzed and classified in a standardized multi-parameter database. Their average abundance was 2.60 × 10^5 items km^{-2} (2.25 × 10^3 to 8.50 × 10^6 km^{-2}) resulting in an estimate of about 650 billion plastic particles floating on the surface of the Mediterranean. This corresponds to an average of 660 metric tons of plastic, at the lower end of literature estimates. High concentrations of plastic were observed in the northwestern coastal regions, north of the Tyrrhenian Sea, but also off the western and central Mediterranean basins. The Levantine basin south of Cyprus had the lowest concentrations. A Lagrangian Plastic Pollution Index (LPPI) predicting the concentration of plastic debris was validated using the spatial resolution of the data. The advanced state of plastic degradation detected in the analyses led to the conclusion that stranding/fragmentation/resuspension is the key process in the dynamics of floating plastic in Mediterranean surface waters. This is supported by the significant correlation between pollution sources and areas of high plastic concentration obtained by the LPPI.

* Corresponding author.
E-mail address: maria-luiza.pedrotti@imev-mer.fr (M.L. Pedrotti).
[1] Equal contribution.

http://dx.doi.org/10.1016/j.scitotenv.2022.155958
Received 28 January 2022; Received in revised form 9 May 2022; Accepted 11 May 2022
Available online 14 May 2022

1. Introduction

Plastic waste pollution has become a major concern. Human discharges of plastics and chemicals into the oceans and continents have now reached a critical point (Persson et al., 2022). It is a priority issue and the G20 countries have committed to reduce further pollution to zero by 2050 (Kato et al., 2021). Still, the global plastic production is growing exponentially, with annual production exceeding 348 million tons, and this quantity is expected to increase tenfold by 2025 (Plastics Europe, 2019). The projected increase in production is, in large part, due to the lack of policies in place to end the use of single-use plastics (Morales-Caselles et al., 2021). Despite current efforts by governments, industry, and society to curb plastic pollution, it has spread worldwide, leading to the emergence of a global problem.

About 8 million metric tons (Mt) of plastic entered the global ocean from land-based sources in 2010 (Jambeck et al., 2015) and according to Borrelle et al. (Borrelle et al., 2020), 19-23Mt of plastic entered aquatic systems in 2016 including rivers and lakes. While these estimates are consistent with annual riverine inputs of 0.8–2.7Mt calibrated from field observations by Lebreton et al. (Lebreton et al., 2017), a recent reanalysis of the data suggests that riverine fluxes are overestimated by two to three orders of magnitude (Weiss et al., 2021). On the other hand, a reassessment of the load of microplastics (MPs <5 mm) floating in the oceans estimates 24.4 trillion MPs representing between 82,000 and 578,000 metric tons (Isobe et al., 2021), which is a significant increase from previous estimates (Cózar et al., 2014; Eriksen et al., 2014). With respect to the Mediterranean, a recent estimate revealed that the total annual load of plastic entering the Mediterranean is approximately 17,600 metric tons and that approximately 3760 metric tons of plastic are currently floating in the Mediterranean which is consistent with previous projections (750–3000 metric tons), (Cózar et al., 2015; Ruiz-Orejón et al., 2016; Suaria et al., 2016). The discrepancy between plastic input and plastic loads floating on the ocean surface, referred to as "missing" plastic problem, remains relevant today and reflects our lack of knowledge about the key processes that bring and selectively remove plastic debris from the surface (Fazey and Ryan, 2016; Lusher et al., 2015). Despite the increase in scientific data on the distribution, quantities, sources, and impacts of plastics in the ocean a proper assessment of mass fluxes from terrestrial and marine sources remains to be achieved (Lebreton et al., 2019; Pabortsava and Lampitt, 2020). Once plastics enter the environment, weathering and fragmentation of larger debris leads to the formation of smaller particles down to the nanometer scale called nanoplastics (Andrady, 2011). In addition, microparticles produced from cosmetic beads, textile fibers, paints, ropes, and tires, enter the ocean directly as MPs (Ryan et al., 2009). These MPs persist in the marine environment because degradation in seawater is particularly slow due to reduced UV exposure and lower temperatures in water compared to land (Jahnke et al., 2017). The longevity of plastics implies that they can be transported over long distances favoring their colonization by various organisms, forming an ecosystem at sea with a specific reservoir of microbes that is still little explored (Scales et al., 2021).

In the Mediterranean Sea, the issue of marine litter has been highlighted since the 1970s and has been of political interest as outlined in the Barcelona Declaration (Declaration, 1995). The Mediterranean Sea is the largest and deepest sea on the planet, with intense economic and tourist activity. The basin is one of the busiest maritime routes in the world, with 30% of the world's maritime traffic and a strong demographic pressure of the 466 million inhabitants around the coastal areas, which constitute an enormous human impact on the environment (UN/MAP, 2017).

Due to the almost closed nature of the Mediterranean Sea, surface flow is not significant and, therefore, a permanent input of waste enters the continental shelf from river mouths, overland flow and winds (Hanke et al., 2013). Plastics represent more than 80% of the marine litter observed and constitute the largest share of floating marine litter, sometimes comprising up to 100% items (Morales-Caselles et al., 2021). Unlike oceanic gyres, where plastic accumulation is predictable based on ocean circulation, the high seasonal variability and the intense mesoscale activity of surface currents in the Mediterranean Sea prevent the formation of stable areas where plastic can concentrate (Millot and Taupier-Letage, 2005). Although models of drift and transport of floating marine debris have proposed areas of seasonal plastic accumulation mainly related to proximity to sources such as large cities and rivers (Liubartseva et al., 2018; Mansui et al., 2015; Zambianchi et al., 2017), inconsistencies exist between these models and field data, in part due to poor sampling coverage of the basin (Cózar et al., 2015; Paper et al., 2016; Ruiz-Orejón et al., 2016).

To date, the majority of studies on spatiotemporal abundance and characterization of plastics have been conducted in the northwestern and west-central Mediterranean (Llorca et al., 2020; Paper et al., 2016) and only a few studies in the eastern basin address polymeric characterization of particles (Adamopoulou et al., 2021; Kedzierski et al., 2022). Furthermore, quantification of plastics is often reduced to total abundance or weight measurements and abundance values do not distinguish fragments of varying size and shape. Because plastics are heterogeneous in nature, plastic surface area has been suggested as a key metric for quantification alongside plastic count data (Rivers et al., 2019).

To contribute this critical knowledge gap, TARA Mediterranean, a large-scale expedition with a cross-disciplinary approach, crossed the entire Mediterranean Sea in 2014 between June 3 and November 8 with the aim to gain a better understanding on the sources, transport, distribution and characteristics of surface floating plastic in the different Mediterranean sub-basins. A systematic and standardized analysis was carried out on the samples from 124 stations allowing the study of geographical distribution, abundance, weight, size, surface, circularity and category of plastic fragments. An important dataset of ~75,000 plastic debris was built and is available for further studies. In addition, a set of 4723 polymer spectra of different size classes of plastics was also constituted (Kedzierski et al., 2019b, 2022).

We tested the hypothesis that the distribution and properties of plastics are not homogeneous across the Mediterranean and that regional differences exist in terms of loads and characteristics of plastics. Knowledge concerning the distributions and properties of plastic debris is essential in assessing the efficacy of existing regional policies in the Mediterranean, and the actions required from producers and consumers to reduce plastic pollution.

2. Materials and methods

2.1. Samples collection and preservation

Surface floating plastics were collected onboard the R/V Tara between June and November 2014 in the framework of the TARA Mediterranean Expedition (https://oceans.taraexpeditions.org/en/tara-mediterranee-expedition/). Plastic debris and plankton were sampled at 154 locations across the basins, in coastal and offshore areas (Fig. 1). Five out of seven main marine Mediterranean ecoregions proposed by Spalding et al. (Spalding et al., 2007) were sampled during the Tara Mediterranean expedition. These were the Alboran Sea, the western Mediterranean Sea, the Ionian Sea, the Aegean Sea, and the Levantine Sea. They have potentially distinct hydrodynamical, biogeochemical and ecological characteristics. To better refine the analyses, the western Mediterranean Sea ecoregion was separated into the Ligurian-Provençal Sea, Tyrrhenian Sea and the other stations in the Balearic, Algerian and Sardinian seas were referred to as the WEST-Med stations. In order not to interfere with an ongoing project we did not sample the Adriatic Sea (DeFishGear.net). Due to legal issues, it was not possible to sample the Gulf of Sidra and the coastal areas of most of the Levantine basin. Geographical coordinates of sampling sites and data are available at Zenodo Data Publisher (https://doi.org/10.5281/zenodo.6551501).

Sea surface temperature and salinity were continuously recorded by a thermosalinograph (TSG, Seabird SBE45) that measured temperature and conductivity at a sampling frequency of 0.1 Hz. A high spectral resolution spectrophotometer (WETLabs ACs) measured at 4 Hz the absorption and attenuation of light from which the concentration of Chlorophyll *a*, particulate organic carbon concentration, and a size parameter for micron-sized

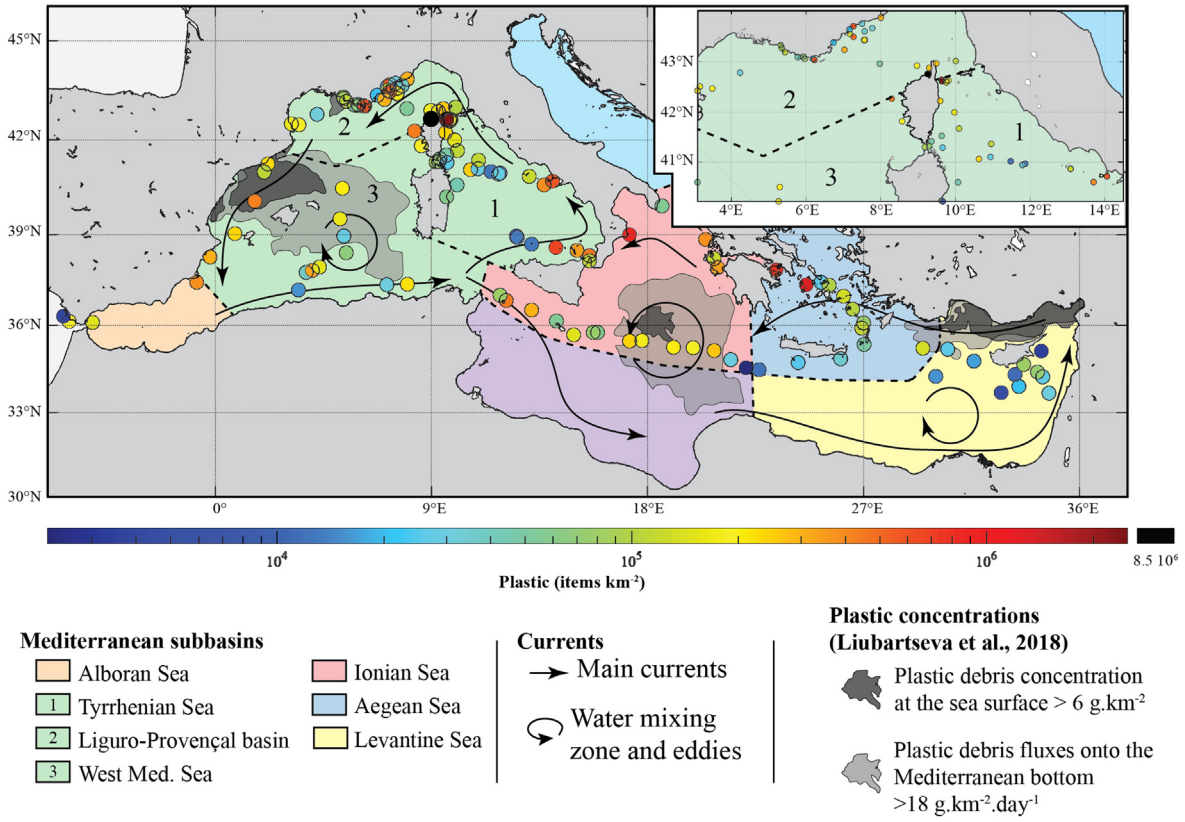

Fig. 1. Concentration of plastic debris (items km^{-2}) collected in surface waters during the Tara Mediterranean expedition. Microplastic concentrations in the different regional basins and the main characteristics of the Mediterranean as defined by Spalding et al. (2007) and the upper layer circulation (Millot and Taupier-Letage, 2005). In light and dark gray are the source, concentration, and flux of microplastics derived from numerical modeling (Liubartseva et al., 2018).

particles were derived as in Boss et al. (Boss et al., 2013). Ocean Colour satellite images supplied by ACRI-ST and Mercator circulation model were combined to determine the zones of interest prior to the sampling.

Samples were collected from the surface using Manta nets (height 25 cm, width 60 cm, mesh size 333 μm) towed at an average speed of 2.5–3 knots for 60 min. This strategy was adopted to sample an appropriate volume of microplastics to reduce the influence of heterogeneous distributions (Hidalgo-ruz et al., 2012; van der Hal et al., 2017). The area sampled was calculated firstly using the towing distance derived from the TSG, synchronized with the vessel's GPS, which gives its position continuously every 10 s. This distance multiplied by the effective mouth net area (0.6 m × 0.16 m) provided the measured volume in cubic meters. We also measured the volume of filtered seawater in each tow using a mechanical flowmeter positioned at the center of the net mouth (Hydro-Bios). Comparisons of the data by the 2 methods showed that the values are significantly correlated with the flowmeter data ($y = 1.59\times$, $r^2 = 0.52$, $p < 0.001$, N 124) underestimating the volumes given by the GPS. This means that plastic abundance was consistently lower with the GPS than with the flowmeter data. We therefore chose to express the results using the distances traveled calculated by the TSG based on the observations made during the survey that the submerged part of the net (0.16 m) always remained in the water filtering the entire sampled area due to the low towing speed of the net thus avoiding possible clogging, backflow and vertical movements of the net. The average surface area sampled was 2640 m^2 per tow and the average filtered volume was 422 m^3. To minimize vertical mixing due to wind (Kukulka et al., 2012), net tows were conducted during periods of calm seas (Beaufort scale 1 to 3) for all sites selected for this analysis. Therefore, they were not corrected to include vertical mixing. In rough weather, we opted to use the Bongo net (300 μm) instead of the Manta net and to collect samples from the subsurface (a total of 30 samples). The data from Bongo net samples were not included in this study. Samples were fixed immediately with a 4% buffered formaldehyde. Sampling did not involve endangered or protected species.

2.2. Sample processing

In the laboratory, the samples were gently transferred to a Petri dish. Plastic-like particles were manually separated from other components such as wood, zooplankton, and organic tissues. We also individually recovered plastics entangled in zooplankton and aggregates during a time-consuming sorting process, for that we used a light box and a dissecting stereomicroscope to ensure the collection of small and transparent debris. The visual criteria used to classify a microfiber as synthetic were the absence of cellular structures and scales on the surface, a curved shape with a uniform surface, the presence of equal thickness along the entire length, spots, and strong strands (Barrows et al., 2018; Hidalgo-Ruz et al., 2018). During processing, microfibers that could not be confirmed as synthetic were discarded. Therefore, in this study, we included a category of synthetic fibers hereafter referred to as “Microfibers” and their abundance and size measurements were included in the results. Each sample was examined twice to ensure the detection of most of the plastic particles. The zooplankton was analyzed separately. To minimize the contamination in our samples, a quality control approach was undertaken following the protocol described by Pedrotti et al. (Pedrotti et al., 2021). All equipment was cleaned with milli-Q and a cotton jacket was worn during sampling and post-processing. During plastic sorting in the laboratory and analysis with the ZoosCan, an ambient air blank was made by placing a cellulose acetate filter (Whatman®) in a clean 47 mm glass Petri dish held open throughout the experiment. The filter was then inspected under stereomicroscopy and the synthetic microfibers, if present, were counted (between 2 and 15 items) and blanks were subtracted from the samples.

2.3. Plastic analysis

The sorted plastic was counted, measured, and weighted. Plastic items were then scanned twice, in black and white and in colour to optimize processing, using the ZooScan Hydroptic system (Gorsky et al., 2010). A total of 75,030 items were analyzed. Particles are automatically detected and their morphological attributes are extracted through post-processing with Zooprocess and Plankton Identifier softwares (Fig. S1). The following parameters were calculated for each particle: the surface area (mm^2), length (mm), the equivalent spherical diameter, the circularity (defined as 4π area/perimeter^2) with values ranging from 0 to 1; 1 indicating a perfectly circular object. The circularity was only given for rigid fragments. By including recovered microplastics entangled with zooplankton and aggregates, microplastics were identified down to a size of 333 μm. Plastics were also semi-automatically classified into six shape categories (rigid fragments, films, foam, granules, rope filaments, and microfibers) through an AI-based machine learning process. Firstly, a dataset corresponding to the typology of each plastic was built. Then the software classifies plastics scanned into different categories based on multiple parameters (as size, transparency, and shape) incrementing the database, and at the end of the process, a human validation corrects the errors in classification. Once digitized, all the plastics particles were transferred to the Ifremer LERPAC laboratory (France) to be re-analyzed following guidelines for monitoring, analysis, and evaluation by the MFSD and GESAMP (Galgani et al., 2013; Kershaw et al., 2019). Briefly, plastics were counted and the three-size fractions (< 5 mm, between 5 and 20 mm, > 20 mm) were dried in an oven at 50 °C for 24 h and weighed on an electronic balance (accuracy: 0.1 mg) and separated in 5 categories using the MFSD protocol. In order to validate the post-processing performed on the plastics typology, for future analyses, we standardized and compared the results obtained with ZooScan and those from visual counts during a two-day workshop.

Plastic concentrations were calculated by dividing the numerical and mass concentration of plastics in each tow by the sea-covered area per tow. The abundance and mass concentration as well as the surface area occupied by plastic debris were expressed in items/km^2 (or items/m^3), g/km^2, and m^2/km^2, respectively. Mean values and lower and upper limits of 95% bias-corrected and accelerated bootstrap (BCa) confidence intervals (CIs) were calculated as well as the mean and confidence interval using the prediction of the "Lagrangian Plastic Pollution Index" (see below). The plastic particles size distribution was determined by separating the plastic items into 94 size classes ranging from 0.330 mm to 62 mm according to the harmonic progression (HP), a mathematical model where the maximum size range calculated for each size class is equal to 1.060*minimum ESD (equivalent spherical diameter) size range, and thus using larger bins as the plastic items get larger. The size distributions were then normalized by the width of the considered size class. Plastic debris were referred to as micro- (≤5 mm), meso- (5 mm to 2.0 cm), and macroplastics (> 2.0 cm), using the standards adopted by UNEP. All results were then uploaded in EcoTaxa http://ecotaxa.obs-vlfr.fr, (Picheral and Irisson, 2017) a free access tool for the taxonomic classification of images (Fig. S1).

2.4. Polymeric composition

To certify the polymeric nature of the collected material, Fourier transform infrared spectroscopy (FTIR) analyses were performed at the Institut de Recherche Dupuy de Lôme (IRDL, Lorient, France). For that, 4723 particles (from 0.315 to 5 mm) from 54 selected sites were analyzed following a computational method developed (Kedzierski et al., 2019a) that provides a representative view of the particle size distribution and chemical nature of the particles, and calculates the associated margin of error. Analyses confirmed that 97% of the MPs particles were synthetic materials, mainly polyolefins, with polyethylene (PE) and polypropylene (PP) accounting for 67.3 ± 2.4% and 20.8 ± 2.1% of the polymers collected, respectively (Kedzierski et al., 2022).

2.5. Statistical analysis

Principal component analysis (PCA) was performed on the concentrations of different plastic categories transformed, using the Hellinger transformation, to investigate the different compositions of the plastic population in the basin. The data set consisted of 124 concentration values (items/km^{-2}) for each of the 6 plastic categories. To understand the extent to which this composition changes with geographic location, each sample was colored using its relative position in the first 3 axes of PCA space using a simple red-green-blue code, which allowed these PCA values to be re-projected directly onto the map. To better understand whether plastic composition is influenced by the environment or by other particle properties (abundance, weight, size fractional abundance, or polymer composition), a posteriori correlation of these external variables with the PCA component was established. Linear regression models 2 and Pearson correlations were used to compare the relationships between plastic category, concentration, weight, surface area, and size. Outliers were detected using Tukey's Hinges percentiles of 25% and 75% and 1.5 × interquartile. The Kruskal-Wallis test using Chi-Square distribution was used to test for differences in plastic concentrations (abundance and weight), plastic area, and sizes between Mediterranean sub-basins. Data from the Alboran Sea do not meet this significance criteria and are not included. Analyses of covariance (ANCOVA) and post hoc tests were carried out to test differences in the plastic size distribution among basins and differences in categories of plastics (data from foams do not meet the criteria and are not included). All analyses were performed using Matlab (TheMathWorks). Normality and homogeneity of variance were checked and the level of statistical significance was set to $p < 0.05$.

2.6. Lagrangian Plastic Pollution Index

In order to understand whether the plastic stock measured at a given station depends on specific sources encountered by the water mass carrying it, we developed a new Lagrangian diagnostic, the "Lagrangian Plastic Pollution Index" (LPPI). The LPPI is calculated by combining the simulated path traveled by the water parcel in the previous days with the land-based plastic sources encountered. Thus, the LPPI estimates the plastic content, which is expected at a given station, and its values are compared with in situ observations. Details of the LPPI calculation are provided below.

2.6.1. Surface area representing the water sampled at each site

We considered 122 out of 124 sites sampled with Manta net because two of them were located outside the Mediterranean Basin, close to Gibraltar, and consequently their positions fell outside the domain of the hydrodynamical field. Each site was characterized by the starting and the final coordinates of the tow. To represent the water mass sampled we considered an around of each transect using a 'stadium' shape (a rectangle with two semicircles on opposite sides). The centers of the two stadium semicircles corresponded to the start and end sampling coordinates of the tow, and had a radius of 0.01°. Each stadium was filled with virtual water particles separated by 0.0025°, for an amount of ~200 virtual particles for each towing site, and the mean value was selected. In this way, we did not extract properties at the specific site location but considered a buffer around them. This choice was made in order to smooth out possible errors in the velocity field (which has a resolution of about 4 km). It was also corroborated by previous studies comparing in situ measurement with model and remote sensing observations (Baudena et al., 2021; Ser-Giacomi et al., 2021). The duration of the Manta sampling is on the order of the velocity field time step (one hour). Therefore, as sampling time T_s of each site, we considered the average of the sampling start and end times.

2.6.2. Velocity field and trajectory calculation

The hydrodynamical velocity field used to simulate the advection was obtained through the combination of two hydrodynamical fields, both downloaded from the Copernicus Marine Environment Monitoring Service

(CMEMS, http://marine.copernicus.eu/). The first product was the MEDSEA_REANALYSIS_PHYS_006_004 (MED_RE), which provides horizontal currents at the surface and includes geostrophic and Ekman components. It has a spatial resolution of 1/16° and is supplied at a daily frequency. The second product was the MEDSEA_HINDCAST_WAV_006_012 (MED_HI), which furnishes the Stokes drift (not provided in MED_RE). It has a spatial resolution of 1/24° and a temporal resolution of 1 h. The two velocity fields were combined as follows: the MED_RE data, which has a temporal resolution of 1 day, were interpolated at an hourly frequency to overlap the temporal resolution of MED_HI. The hourly interpolations of the MED_RE data were then spatially interpolated on the grid of the MED_HI. These two fields were then added together, giving the final velocity field, which therefore has a spatial resolution of 1/24° and a temporal resolution of 1 h. This combination allowed us to consider the geostrophic component, the Ekman effect, and the Stokes drift, which implicitly considers the windage effect. This choice is supported by recent Lagrangian models built specifically for the Mediterranean basin considering the importance of the effect of Stokes drift in plastic debris transport (Baudena et al., 2022; Liubartseva et al., 2018). Backward advection was computed with a 4th order Runge-Kutta scheme, with a time step of 0.5 h.

2.6.3. Terrestrial sources of plastics

Plastic debris is considered to enter the marine environment from two main land-based sources: cities and rivers. Even though plastic debris generated in cities may reach oceans via rivers, information about how to express city and river contribution together is lacking. Therefore, we consider them separately, in agreement with previous studies (Baudena et al., 2022; Liubartseva et al., 2018). Usually, city and river relative contribution to the total flux of plastic entering the oceans is estimated to be $p_c = 40\%$ and $p_r = 40\%$ respectively (Lebreton et al., 2012; Li et al., 2016) while the rest (20%) is expected to originate from ships. Based on recent studies (Baudena et al., 2022; Liubartseva et al., 2018; Soto-Navarro et al., 2020) we changed these values to $p_c = 50\%$ and $p_r = 30\%$.

Here, we define the *Plastic Emission Probability* of each land-based source as follows.

2.6.3.1. Cities. Cities with more than 50,000 inhabitants and less than 20 km from the coast were selected, for a total of 185 cities. The positions and populations of the cities, updated for 2015, were downloaded from the Urban Cities Database of the Global Human Settlement database. This dataset also provided the outline of each city, which was used to identify the city location along the coast. The *Plastic Emission Probability* of each city was obtained by multiplying its population, the rate of mismanaged plastic waste of its country (Jambeck et al., 2015), the percentage of relative city contribution p_c (50%), and finally by normalizing it. The following formula was employed:

$$PEP_{C_i} = \frac{pop_i \cdot MPW(country_i)}{\sum_{i=1}^{N_{cities}} pop_i \cdot MPW(country_i)} \cdot p_c/100 \quad (1)$$

where PEP_{Ci} is *Plastic Emission Probability* of the *i*-th city, pop_i is the population of the *i*-th city, and MPW (*country*) is the mismanaged plastic waste rate of the country where the city is found. This formulation has been used in a recent model validated with in situ observations (Baudena et al., 2022) to quantify the number of plastic particles released by cities.

2.6.3.2. Rivers. We used the estimates of plastic entering the Mediterranean Sea by rivers (plastic river input PRI) calculated by Lebreton et al. (Lebreton et al., 2017). From this data set, we consider the first 200 Mediterranean rivers for the amount of plastic injected into the sea, as they contribute approximately to 99.3% of the total amount of plastic entering the Mediterranean from rivers.

The *Plastic Emission Probability* of the *i*-th river PEP_{Ri} was obtained by normalizing its plastic river input PRI_i and multiplying it with the percentage of relative river contribution ($p_r = 30\%$):

$$PEP_{R_i} = \frac{PRI_i}{\sum_{i=1}^{N_{rivers}} PRI_i} \cdot p_r/100. \quad (2)$$

2.6.4. Lagrangian Plastic Pollution Index calculation

Virtual particles representing the water mass sampled at each of the sites were advected backward from T_s until a time T_s-τ, with τ varying from 0 to120 days (see below). 120 days was chosen as limit for the backward simulation as (i) the reliability of the hydrodynamical field to properly describe particle trajectories decreases with time (ii) plastic debris fate on longer time scales is affected by dynamics other than transport, such as biofouling, beaching, washing-off, fragmentation, etc. Trajectories positions were saved with a 6 h timestep. Beached trajectories were excluded from the analysis.

For each virtual particle, we compute its LPPI as follows. For each point of the trajectory of the virtual particle: (a) we counted the terrestrial sources (defined in Section 2.6.3) falling below a distance threshold d_t from the point. We considered these sources as being "encountered" by the virtual particle, and therefore potentially contributing to its plastic pollution. Then, (b) we summed the *plastic emission probabilities* (Section 2.6.3) of each source encountered. This was repeated for all the points of the trajectory, and the *plastic emission probabilities* summed together. Finally, (c) the LPPI of a site was calculated as the average of the LPPIs computed for all virtual particles within the shape of the stadium surrounding the site.

Thus, the Lagrangian diagnostic obtained considers (i) whether a water mass has come into contact with a terrestrial source in the preceding days (defined by the interval τ), (ii) the magnitude, in terms of *plastic emission probability*, of the source (or sources) encountered backward, (iii) the time spent in vicinity of the source (or sources). The LPPI index depends on two parameters: the distance threshold d_t necessary to consider a source as "encountered" by the water particle, and the time of backward advection τ. The distance thresholds tested ranged from 0.025° to 2°. The τ employed varied between 0 and 120 days backward in time.

We also computed two complementary indices, the Lagrangian Plastic Pollution Indices for cities and for rivers (LPPIC and LPPIR, respectively) that report the plastic contribution of cities and rivers only, respectively. Another LPPI, calculated by considering vessel density, which is considered proportional to the amount of plastic discarded by vessels (Lebreton et al., 2012) did not show a significant correlation with the Manta station measurements and was not considered in this study.

2.6.5. Bootstrap test

LPPI values were splitted in two groups according to a threshold, fixed at the 75 percentiles of the LPPI distribution. A Mann-Whitney or *U* test was used to test the statistical independence of the two groups. Subsequently, the bootstrap test was applied following the methodology (Baudena et al., 2021). This allowed us to estimate the probability that the difference between the in situ plastic concentrations, over and under the LPPI threshold, was significant and not the result of statistical fluctuations.

3. Results

3.1. Plastic concentrations, types and environmental variables

The median abundance of plastic debris over the entire survey was 1.07 10^5 items km^{-2}. The average was 2.60 × 10^5 items km^{-2} (lower and upper BCa confidence intervals: 1.74 × 10^5 and 5.61 × 10^5 items km^{-2}, respectively; Table 1). The abundance ranged over three orders of magnitude across the entire basin, from 2.25 × 10^3 items km^{-2} in the easternmost part of the basin to a maximum of 8.50 × 10^6 items km^{-2} in the Corsica Channel in the border between the Tyrrhenian Sea and the Ligurian

Table 1
a) Average concentration of all plastic debris collected in surface waters during the Tara Mediterranean Expedition. b) Mean concentration of plastic debris predicted for the entire Mediterranean Sea, in billions of items and in tons, calculated using the Bootstrap method (BCa). CIs are the confidence intervals. c) Same as in (b), but using the LPPI model.

Size		a- Tara Observations				b- BCA Prediction over the Med			c- LPPI Prediction over the Med		
		BCA lower CI	Mean value	BCA upper CI		BCA lower CI	Mean value	BCA upper CI	BCA lower CI	Mean value	BCA upper CI
All	Plastic abundance	1.74	2.60	5.61	Plastic Prediction	435	650	1403	259	470	680
0.3-1 mm	(items 10^5 km^{-2})	0.81	1.22	2.56	(billions of items)	203	304	639	–	–	–
<5 mm		1.64	2.48	5.61		411	621	1404	–	–	–
5–20 mm		0.04	0.08	0.26		9.49	20.95	65.28	–	–	–
>20 mm		0.001	0.002	0.004		0.33	0.51	0.91	–	–	–
All	Plastic weight (g km^{-2})	179	264	450	Plastic Prediction (tons)	447	660	1125	–	–	–
<5 mm		49.9	62.5	80.6		125	156	202	47	135	223
5–20 mm		47.9	59.9	76.1		120	150	190	–	–	–
>20 mm		69.1	141.8	317.5		173	354	794	–	–	–
All		0.72	0.97	1.46		1.80	2.43	3.64	–	–	–
Fragment category	Plastic surface area (m^2 km^{-2})	0.52	0.70	1.18	Plastic Prediction (km^2)	1.31	1.74	2.74	–	–	–

Sea (Fig. 1). Areas identified as having high plastic concentration (greater than 5 × 10^5 items km^{-2}; 90th percentile) were the coastal areas from Nice to Toulon (Ligurian Sea), northern East Sicily, Messina Channel, and Naples coasts (Tyrrhenian Sea), the Gulf of Taranto (Ionian Sea), and the Saronic Gulf (Aegean Sea). In addition, significant amounts of plastics were found between Sardinian Sea and the Balearic Islands (average 2.6 × 10^5 items km^{-2}, WEST-Med) and from eastern Tunisia to southeastern Crete (average concentration over a 15-station transect: 3.7 × 10^5 items km^{-2}, 82.13 g km^{-2}, Ionian Sea). During the expedition we sampled the north-western African coastal zone where the concentration of plastic debris was highly variable in abundance and mass (0.16 to 3.34 × 10^5 items km^{-2}; 3 to 488 g km^{-2}). Relatively less polluted areas (less than <1.6 10^4 items km^{-2}; 10th percentile) were identified further west of Sicily, south of Crete (Ionian Sea), south and east Cyprus (Levantine Sea) and in near the Gibraltar strait (Atlantic station) (Fig. 1). Average abundances of micro-, meso-, and macroplastics in the Mediterranean were respectively 2.48 × 10^5, 8.38 × 10^3, 2.02 × 10^2 items km^{-2} corresponding to 97.70%, 2.21% and 0.09% of all the plastic debris collected (Table 1).

The median mass concentration of plastic particles in the study area was 86.4 g km^{-2}. The average abundance was 264 g km^{-2} (lower and upper BCa confidence intervals: 179 and 450 g km^{-2}, respectively), with a very high spatial heterogeneity, spanning four orders of magnitude (Fig. 2 a, Table 1). The highest mass concentration values were observed in the Bay of Marseille (5340 g km^{-2}), which is explained by the fact that 93% of the total weight of the debris mass was in the macroplastics category (Fig. 2 b). Other areas with high mass concentration were the Corsica channel (4260 and 2380 g km^{-2}), the coastal area of Naples (1730 g km^{-2}), Barcelona (951 g km^{-2}) and one station in the Strait of Gibraltar (1010 g km^{-2}). The lowest mass values were located in the vicinity of Cyprus

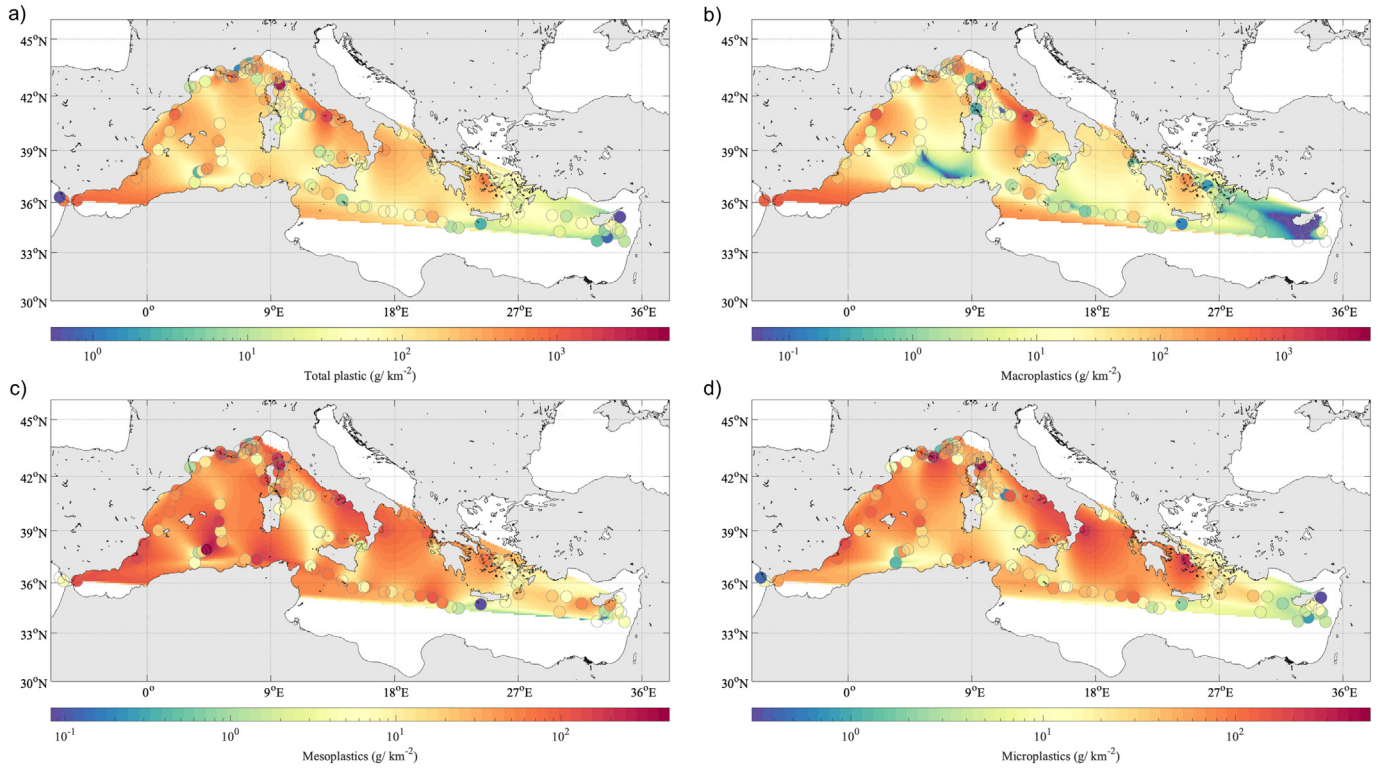

Fig. 2. Concentration of plastic debris (g km^{-2}) collected in surface waters during the Tara Mediterranean expedition. a) total mass concentration, b) macroplastics (size >20 mm), c) mesoplastics (5 < size <20 mm), d) microplastics (size <5 mm).

(0.31 g km^{-2}). The average mass of micro-, meso- and macroplastics in the Mediterranean was 63, 60 and 142 g km^{-2}, corresponding respectively to 46.6%, 34.1% and 19.3% of the total plastics collected (Table 1). The individual weight of a micro-, meso-, and a macroplastic was on average 0.3 mg, 5.8 mg, and 83.2 mg, respectively. The average sea surface area occupied by plastic debris in the basin was 0.97 m^2 km^{-2} (BCa confidence intervals: 0,72 and 1.46 m^2 km^{-2} respectively; Table 1). It corresponded to 0.11 m^2 km^{-2} in the Levantine Sea and increased to 2.62 m^2 km^{-2} in the Tyrrhenian Sea (Table 2 and Fig. S2).

There was no significant variation in plastic abundance as a function to distance to land ($p = 0.29$). Although coastal stations up to 7 miles displayed higher concentrations 4.56 ± 2.78 10^5 items km^2 (N46) than stations offshore in the strip of 50 miles with 1.48 ± 1.53 items km^2 (N59) and > 50 miles with 1.14 ± 1.05 items km^2 ($n = 19$). Significant correlations were found between plastic abundance (item km^{-2}) and total surface area of plastic (m^2 km^{-2}), ($r^2 = 0.91$; $p < 0.001$; N 124) and plastic abundance and plastic weight ($r^2 = 0.72$; $p < 0.001$; $n = 122$), (Fig. 3a and b). Total plastic area was also correlated with plastic weight (g km^{-2}), ($y = 0.007 \times {}^{0.86}$, $r^2 = 0.86$, $p < 0.001$; n = 122). However, some outliers were observed when plotting the results of total plastic weight with other parameters, implying that the use of a single quantification parameter may lead to misinterpretation of the extent of plastic contamination.

The latter relationship was compared to those observed in the open oceans (Cózar et al., 2014), Although the differences are small, they are probably related to processing and sampling methods. This work includes microfibers although the former discarded them when present in the samples. Microfibers significantly increased the total plastic number in the samples, but they contribute little to the total weight. Moreover, we included plastics entangled with zooplankton and aggregates, mainly recovering relatively small particles such as fibers. In contrast, Cózar et al. (2014) did not make a special effort to collect these plastic particles. These are key factors for the size of the plastic particles observed. We have given the percentage of fibers separately (Fig. S3) as well as the concentrations of plastics without fibers and the concentrations of fibers (items km^{-2}), (Fig. S4).

In the western basin (65% of the sampled sites), 70% of the stations have a plastic mass > 50 g km^{-2}, while in the eastern basin this percentage drops to 14%. An increase in the contribution of MPs to the total plastic mass (53.8%) and a decrease in the contribution of macroplastics (11.7%) were observed towards the eastern basin, while mesoplastics show comparable values in the 2 basins. As a result, the surface to mass ratio of plastics is greater in the eastern basin (mean 3.10), with decreasing values towards the western basin (mean 1.78).

At the sub-basin level, significant differences were observed in the amounts of plastics (Table 2, Table S1). The Levantine Sea has significantly lower abundances than the other 5 sub-basins (Kruskall-Wallis H $\chi 2 = 17.15$, $p = 4.23 \times 10^{-3}$), which do not show significant differences between them. The plastic mass was not homogeneous between the sub-basins with comparable values between the Levantine and Aegean Seas, which they are lower than the other 4 sub-basins that have comparable values (Kruskall-Wallis H $\chi^2 = 23.04$, $p = 3.31 \times 10^{-4}$). The surface area occupied by plastics follows the same pattern as the distribution of plastic mass (Kruskall-Wallis H $\chi^2 = 22.64$, $p = 3.95 \times 10^{-4}$).

Considering the approximate surface of the Mediterranean Sea being 2.51 million km^2, we estimated that it likely contains a total of 650 billion pieces of plastic debris floating on its surface (BCa confidence intervals: 435 and 1403 billion pieces, respectively; Table 1). Considering only particles <5 mm, it represents 621 billion pieces. The total load is 660 tons (BCa confidence intervals: 477 and 1125 tons, respectively). The total surface occupied by plastics is 2.43 km^2 (BCa confidence intervals: 1.80 and 3.64 km^2, respectively); considering the surface area only for fragments (hard plastic objects) we obtained 1.74 km^2 (BCa confidence intervals: 1.31 and 2.79 km^2, respectively).

Plastic typology analyzed by ZooScan showed that hard plastic fragments objects were the most common forms of non-fibrous MPs averaging 81% of all collected plastics, with the Ionian Sea having the highest percentage (86.8%) and the Levantine Sea the lowest (70%). Films (e.g., pieces of bags or packaging) represented on average 2.6%, with the Levantine Sea

Table 2
Median and mean plastic concentrations (km^{-2}, m^{-3}, g), total surface area occupied by plastics (m^2 km^{-2}), size length (mm) and surface area of particles in the different sub-basin of the Mediterranean Sea. Differences among basins were detected by the Kruskal-Wallis tests using Chi-Square distribution with multiple pairwise comparisons. In red are underlined the significant differences between the sub-basins (see Table S1).

Bassin		Alboran	Tyrrhenian Sea	Ligurian-Provençal	WEST Med	Ionian Sea	Levantine Sea	Aegean Sea
Plastic abundance (items 10^5 km^{-2})	median	*1.71*	*1.15*	0.93	1.68	1.69	*0.21*	*1.02*
	mean	1.85	4.69	1.63	1.67	2.08	0.29	2.49
	std	(± 1.61)	(± 1.36)	(± 1.81)	(± 1.21)	(± 2.10)	(± 0.26)	(± 4.10)
	n	*4*	*35*	*25*	*17*	*20*	*11*	*12*
Plastic abundance (Items m^{-3})	median	*1.07*	*0.72*	*0.56*	*1.15*	*1.06*	*0.13*	*0.64*
	mean	1.15	2.93	1.02	1.18	1.30	0.18	1.56
	std	(± 1.0)	(± 9.11)	(± 1.1)	(± 0.84)	(± 1.31)	(± 0.16)	(± 2.56)
	n	*4*	*33*	*22*	*17*	*20*	*11*	*12*
Plastic weight (g km^{-2})	median	524.81	88.1	175.18	149.05	83.75	11.9	42.15
	mean	514.68	380.18	395.87	231.18	127.15	19.66	97.20
	std	(± 425.00)	(± 850.52)	(± 1043.48)	(± 236.22)	(± 120.97)	(± 22.43)	(± 166.10)
	n	*4*	*33*	*25*	*17*	*20*	*11*	*12*
Total plastic surface area (m^2 Km^{-2})	median	*0.70*	0.53	0.73	0.58	0.54	*0.90*	0.30
	mean	0.73	2.60	0.890	0.67	0.94	0.11	0.74
	std	(± 2.59)	(± 0.88)	(± 1.04)	(± 1.26)	(± 1.16)	(± 1.56)	(± 1.50)
	n	*4*	*35*	*25*	*17*	*20*	*11*	*12*
Plastic median lenght (mm)	mean	1.11	1.14	1.17	1.12	1.25	1.18	1.17
	std	(± 0.16)	(± 0.05)	(± 0.06)	(± 0.08)	(± 0.07)	(± 0.10)	(± 0.09)
	n	*4*	*35*	*25*	*17*	*20*	*11*	*12*
Plastic surface area (mm^2)	mean	3.70	8.05	8.39	6.30	5.10	4.93	5.30
	std	(± 3.82)	(± 1.29)	(± 1.53)	(± 1.85)	(± 1.71)	(± 2.30)	(± 2.21)
	n	*4*	*35*	*25*	*17*	*20*	*11*	*12*

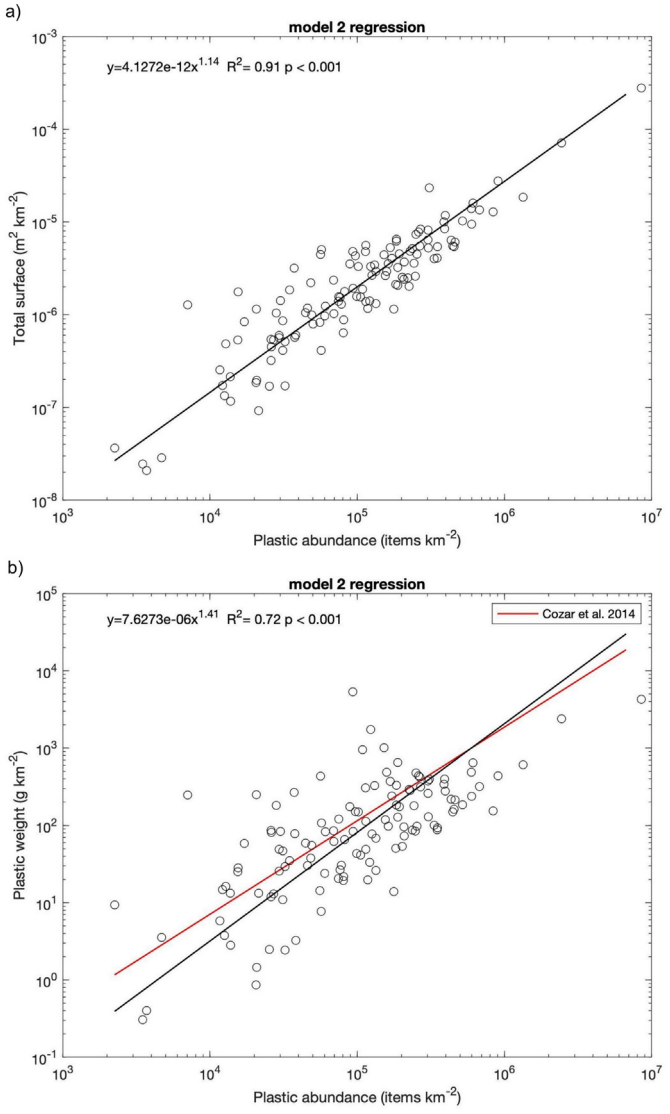

Fig. 3. Regression Model 2 with scatter plot showing the relationships between a) plastic abundance (item km^{-2}) and plastic total surface area (m^2 km^2) (r^2 = 0.91; $p < 0.001$; $n = 124$), b) plastic abundance and plastic weight (g km^{-2}) (r^2 = 0.72; p < 0.001; $n = 122$), during the Tara Mediterranean expedition. Overlaid in red are the results of Cózar et al. (2014) for the open ocean. Black line shows the log-log linear-square fitting on the dataset.

having the highest percentage (6.5%) and the WEST-Med and Alboran basin the lowest (1.8 and 1.2%). Filaments (e.g., ropes, fishing lines) accounted for 2.8% of total debris, with the Levantine Sea having the maximum percentage (6.3%) while in the other sub-basins exhibited comparable values (2.2- to 2.7%). Foam and pre-production plastic pellets/granules were present in lower proportions (0.7 and 1.0%) throughout the basin (Fig. S3). The concentration of Microfibers accounted for 11.2% of all plastics collected, with the Levantine Sea showing the highest percentage (16.5%) and the Ionian Sea the lowest (7.8%), while the other sub-basins showed comparable percentages (10–12%). The abundance of microfibers in our samples was significantly correlated with the abundance of total plastic ($r = 0.9, p < 0.0001$, Fig. S5a) and with the abundance of synthetic microfibers (SFPs) collected simultaneously from 10 stations and filtered through a 20 μm sieve ($r = 0.868\, p < 0.001$; $n = 10$) and reported in Pedrotti et al. (2021), (Fig. S5b). Comparisons between ZooScan and visual analysis showed that the film categories are underestimated by ZooScan, that likely includes 4% of total films in the fragment category, however the percentages between sub-basins do not change.

During the cruise, temperature and salinity in Mediterranean waters ranged from 17.12 to 28.60 °C and 35.66 to 38.35 PSU respectively, showing a seasonal gradient from spring to late summer and increased oligotrophy from west to east. PCA analysis performed on particle properties (abundance, weight) with a posteriori correlation of environmental variables (T°C, salinity, particulate organic carbon (POC), gamma- optical size parameter) and polymer composition (Kedzierski et al., 2022), showed that areas of low plastic abundance were correlated with low chlorophyll, low particulate organic carbon (POC) concentrations, and an eastward longitudinal gradient (Fig. 4a). The PCA performed on the concentrations of the different plastic categories and their geographical distribution produced a two-dimensional diagram with axis 1 (40%) representing the concentrations of Microfibers present throughout the basin in contrast to the other plastic types. Axis 2 represents the concentrations of the other plastic categories, with films and filaments present in greater concentration towards the east of the Mediterranean and fragments in greater concentration towards the west (Fig. 4b and c). In addition, the presence of polyethylene was significantly correlated with a higher proportion of fragments and polyamide and polystyrene were correlated with the presence of Microfibers (Fig. 4a and b).

3.2. Size distribution and circularity of plastic debris

ZooScan-derived individual particle analysis showed that the median length of all collected plastics was 1.04 mm (mean 1.43 mm). The median length of micro-, *meso*-, and macroplastics was respectively 1.02, 6.72, and 25.2 mm. The median surface area of plastic debris was 1.05 mm^2 (mean 4.45 mm^2). The median surface area of micro-meso and macroplastics was respectively 1.0, 43 and 609 mm^2 (Table 3). The circularity for the typology of plastic fragments derived from ZooScan data, varies from 0.05 to 0.90 with the mean value of 0.424; CI 5% 0.422 –0.425. Circularity correlates with the length of plastic fragments with a significant increase with decreasing particle size (Spearman rank correlation $r = -0.564$, $p < 0.001$, $N = 64{,}967$). The cumulative size frequency distribution (for all 75,030 particles) skewed towards the lower size range with an increase in particle number with decreasing size and a strong correlation between micro and mesoplastic abundance (y = 0.0597× - 6662.7; $r = 0.95$, p < 0.001). Indeed, a gradual increase in abundance towards the size of 1 mm was observed, followed by a flattening of the slope below 1 mm. Among microplastics, the size class]1–0.3 mm] mm was the most abundant (48.8%; of the collected microplastic objects), followed by the size class] 2–1 mm] and]5–2 mm] (34.4% and 16.8%, respectively).

Based on these results, we separated the particle size distribution (PSD) into two regression-fitted curves and estimated the slopes of the power-law model (Fig. 5a). The overall size distribution of items ≤1 mm scales with an exponent $\alpha = -0.37$ and those of plastics >1 mm with $\alpha = -1.96$. The associated values of the coefficients of determination were quite high (r2 = 0.99 and 0.75 respectively, $p < 0.002$) and suggest that this model can explain different patterns regarding fragmentation and loss processes. At the sub-basin scale, ANCOVA analysis showed significant differences for both plastic size distribution curves (Fig. 5b, Table S2). The power law exponent for each sub-basin provides information on the relative concentration of small versus large plastic debris. The steeper the slope in absolute value, the greater the proportion of small particles. For the size class debris ≤1 mm (F = 143.26; $p = 1.34$–93) the slope of the Levantine Sea differs significantly from that of the Aegean Sea, Alboran Sea and WEST Med, while the other sub-basin does not show significant differences between them. For debris >1 mm (F = 322.48; $p = 1.72^{-77}$) the slope of the Levantine Sea differs significantly from the slopes of the other 6 basins. In addition, the Ligurian Provençal basin has a significantly different slope from the Aegean, Alboran and WEST-Med and the Aegean Sea has a different slope from the Ionian Sea and Tyrrhenian. (Table S2). Power-law regressions were fitted to the size distribution of the different plastic categories and ANCOVA analysis showed that the slopes differed significantly according to the type of plastic (Fig. 5c). For items ≤1 mm (F = 231.07; $p = 1.94^{-46}$) Microfibers have slopes significantly different from the others

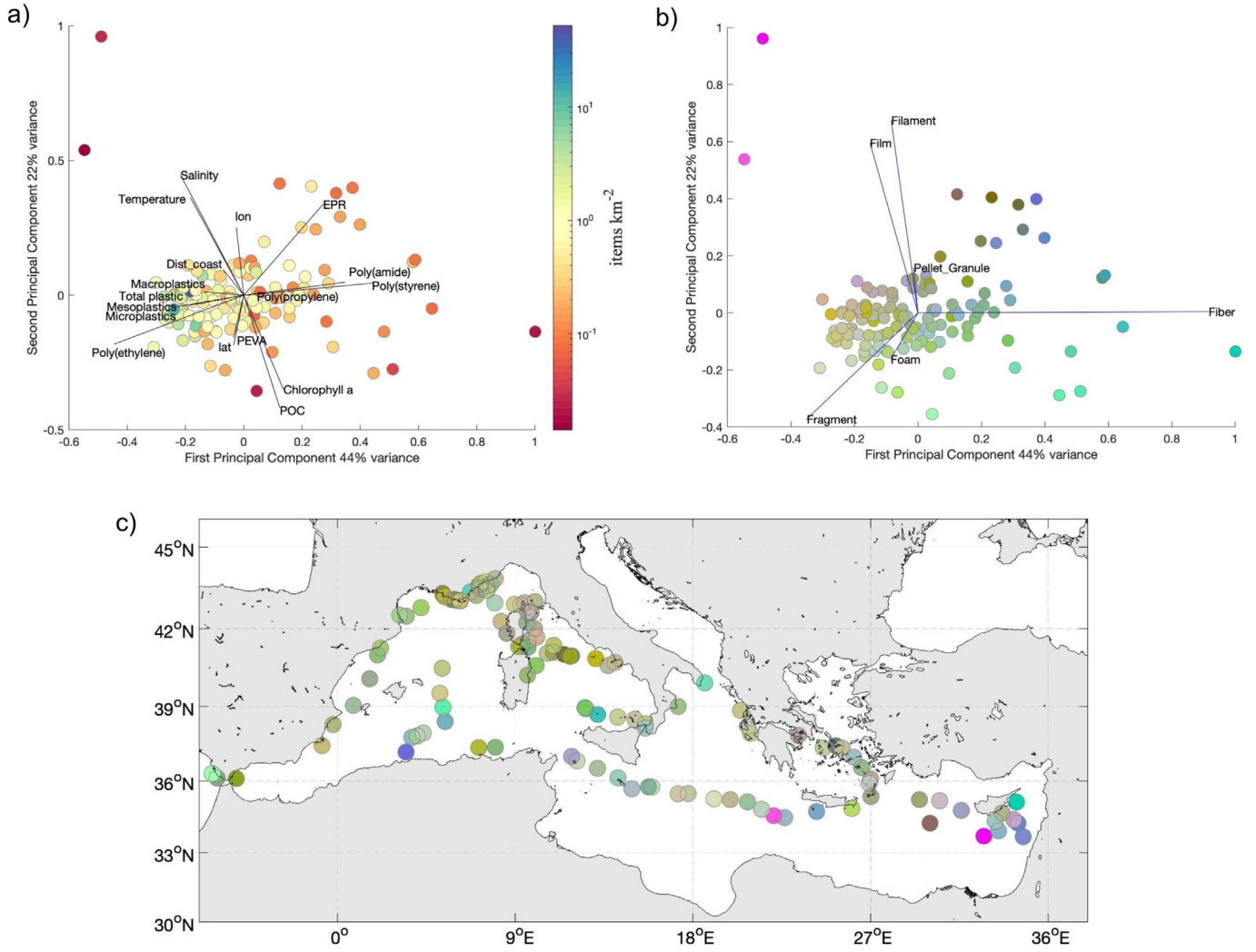

Fig. 4. a) Principal Component Analysis (PCA) with ordination of samples performed on the particle properties (abundance, weight) with a posteriori correlation of environmental variables (T°C, Salinity, particulate organic carbon (POC), gamma) and polymer composition (Kedzierski et al., 2022).b) PCA performed on the concentrations of different plastic categories and their geographical distribution c) To understand the extent to which this composition changes with geographic location, each sample was colored using its relative position in the first 3 axes of PCA space using a simple red-green-blue code, which allowed these PCA values to be re-projected directly onto the map.

categories as well as filaments, while fragments, films and pellets, have similar slopes. For items >1 mm ($F = 224.85$; $p = 7.52^{-77}$), fragments have slopes significantly different from the others categories, pellets have slopes significantly different from filaments and films (Table S3).

3.3. Validation of the Lagrangian Plastic Pollution Index with Manta plastic observations

We assessed whether the amount of plastic debris sampled during the Tara Mediterranean expedition could be associated with the history of the water parcel sampled. For this reason, the waters from the 122 Manta sites were tracked through a backward advection, and their Lagrangian Plastic Pollution Index (LPPI) calculated (details in Section 2.6). We used an advection time $\tau = 15$ days, and a distance threshold from land-based plastic sources $d_t = 0.2^{\circ}$. The LPPI values were compared to the measured plastic concentration, using both the plastic mass (g km^{-2}) and the number of plastic items (items km^{-2}). Results showed a significant correlation of the LPPI with mass and number of collected plastics debris (Fig. 6a; $r = 0.41$ and 0.59; $p < 0.01$ respectively). In addition, the bootstrap test showed that the plastic mass and the number of plastic items were significantly higher in stations with larger LLPI (Fig. S6; $p < 0.05$; $p < 0.001$ respectively). These relationships were present for 34 sites with a non-zero LPPI, i.e., the sites where the water had passed near a land-based plastic source in the previous τ days. To test the robustness of the results, the R and significance were calculated repeatedly for incremental changes in the advection time τ used to calculate the LPPI (between 0 and 120 days backward in time). The correlation between the plastic concentration measurements and the LPPI was significant for advection times between 5 and 15 days (Fig. 6b), as well as the bootstrap test (Fig. S6). When decreasing the distance threshold d_t to 0.05°, the correlation was significant for a large range of advection times, between 5 and 95 days, depending whether the plastic concentration was expressed as mass or number of items

Table 3
Average size (mm) and surface area (mm^2) of the plastic debris collected during the Tara Mediterranean expedition.

Size	ESD (mm)				Area (mm^2)			
	Mean	Median	Min	Max	Mean	Median	Min	Max
All	1.43	1.04	0.15	61.97	4.45	1.05	0.07	3493.16
0.3-1 mm	0.61	0.61	0.15	1.00	0.41	0.35	0.07	2.18
<5 mm	1.26	1.02	0.15	5.00	2.29	1.00	0.07	45.34
5-20 mm	7.71	6.72	5.00	19.98	65.29	43.80	20.18	404.57
>20 mm	28.70	25.52	20.44	61.97	841.08	609.98	359.06	3493.16

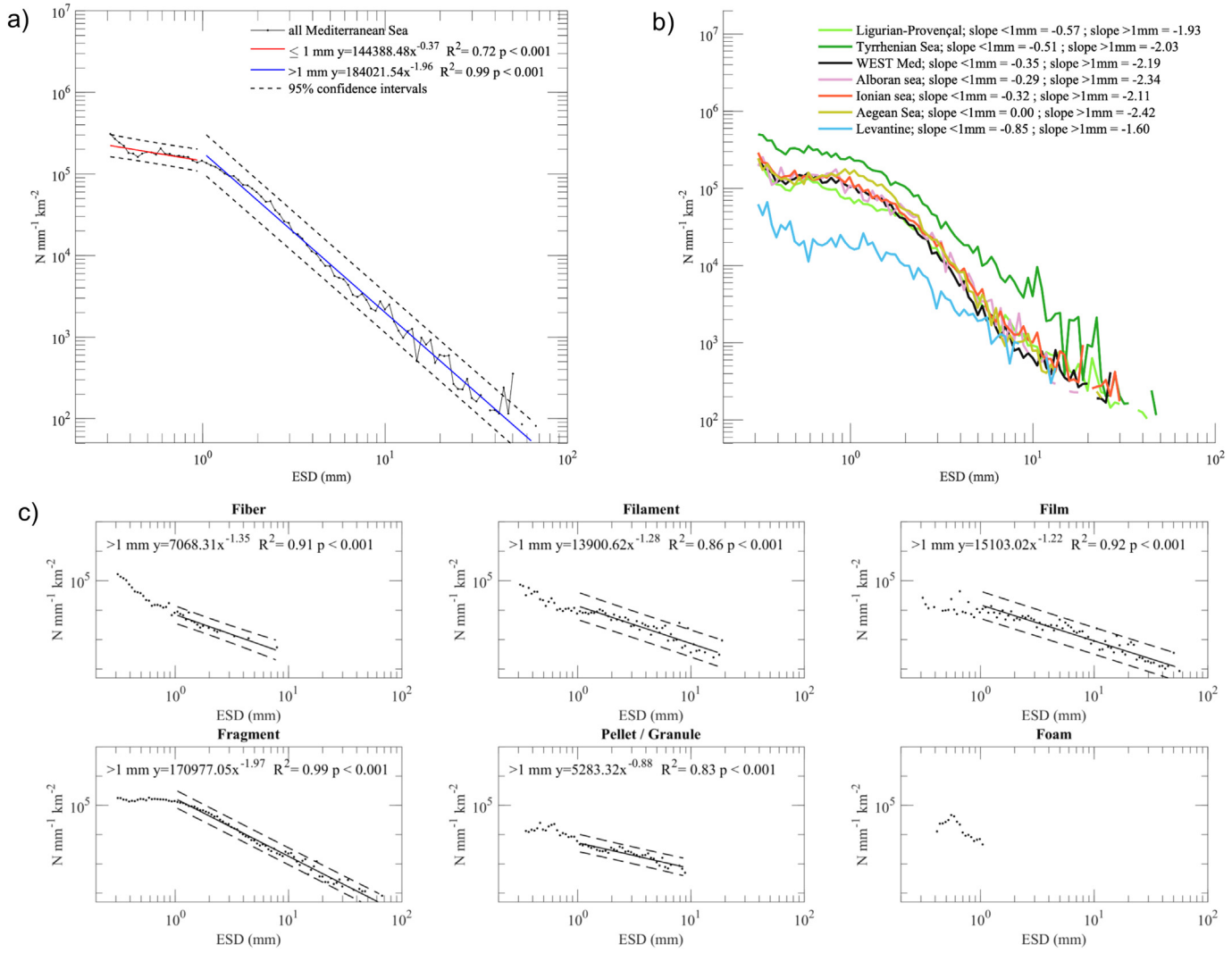

Fig. 5. Size distribution of plastics fitted to a power-law regression a) overall size distribution of 75,030 plastics for particles >1 mm and ≤ 1 mm. The solid blue and red lines show the fit of the logarithmic regression model used to estimate the slope of the PSD over the 2 selected size ranges. b) size distribution of sub-basins for plastics >1 mm and ≤ 1 mm C) size distribution for different plastics typologies. Black dot line shows the 95% confident interval.

(Fig. S7). When the pollution index is calculated using only cities (LPPIC) or rivers (LPPIR), the significance is confirmed (Fig. S8). These results show that the LPPI is a robust diagnostic that can be used to predict plastic concentrations across the basin (Table 1). An LPPI was also calculated by considering vessel density, considered as proportional to the amount of plastic discharged by vessels (Lebreton et al., 2012). However, this index did not show a significant correlation with our measurements. This can be due to the different nature of debris released by vessels and to the relatively coarse resolution of the vessel density product (1/6°).

4. Discussion

4.1. Dynamics of plastics in the Mediterranean

Our measurements suggest that the Mediterranean plastic debris is in a more advanced stage of degradation than those detected in several areas of the Pacific and the Atlantic oceans. They have a smaller size, a smaller surface area, and a lighter mass (Cózar et al., 2014; Goldstein et al., 2013; Morét-Ferguson et al., 2010; Rivers et al., 2019). Comparison of PP/PE ratio in Kedzierski et al. (Kedzierski et al., 2022) with that of Enders et al. (Enders et al., 2020) seems to point to a more advanced segregation process in the Atlantic (PP/PE = 0.14) than in the Mediterranean Sea (PP/PE = 0.31). This could mean more regular inputs of microplastics in the Mediterranean Sea than in the central Atlantic Ocean, or a shorter drift time at the surface of the marine environment. Other regional scale studies in the Mediterranean, although more coastal, have also reported an average size and surface area of plastic in agreement with our results (de Haan et al., 2019; Pedrotti et al., 2016; Ruiz-Orejón et al., 2016).

The surface-to-perimeter ratio (circularity) is also lower for small plastics, suggesting that large marine debris with irregular edges are eroded progressively to smaller and more round forms through mechanical degradation. The same relationship was also found in the California Current system and was attributed to a long residence time of the particles in the ocean undergoing weathering and getting rounder in shape (Gilfillan et al., 2009). When analyzing the surface of the fragments collected during the Tara Mediterranean expedition, almost all MPs showed multiple cracks and roughness on the surface indicating that they had undergone photodegradation and/or aging processes (Fig. S9). However, in the Mediterranean, the residence time of plastics in surface waters is estimated to be relatively short, between 7 and 90 days (Baudena et al., 2022; Liubartseva et al., 2018), so such a degraded state is difficult to explain by a long residence time in the water. Given the limited area of the basin and the lack of long-term accumulation (Cózar et al., 2015; Mansui et al., 2015), an alternative explanation is an input of MPs in a more advanced state of fragmentation from

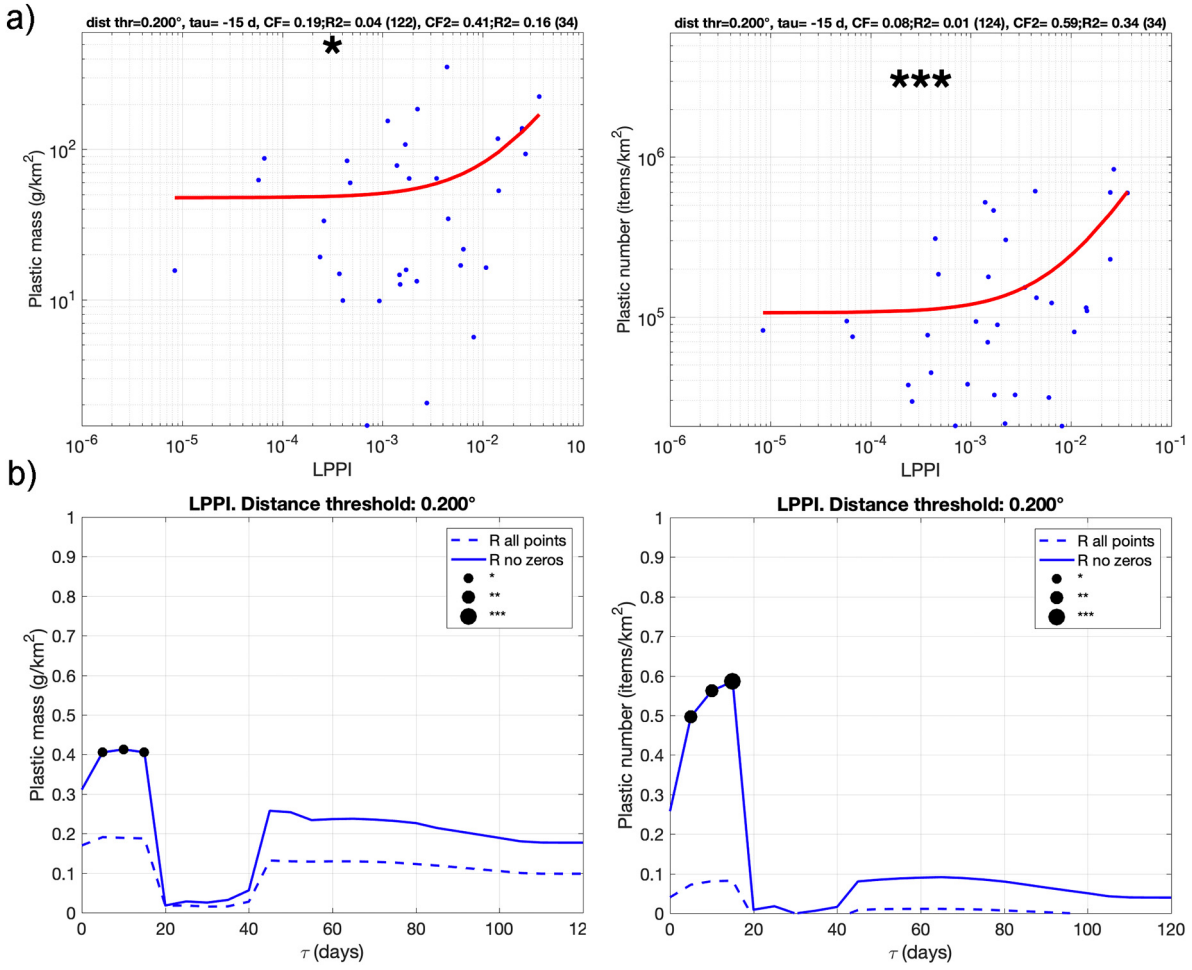

Fig. 6. a) Plastic concentration (y-axis; g km^{-2} and items km^{-2}, left and right panels, respectively) versus Lagrangian Plastic Pollution Index (LPPI, x-axis) in the 34 sites where LPPI ≠ 0. For the LPPI computation, the advection time τ used was −15 days and the distance threshold dt = 0.10°. The red lines represent the result of the linear fit. Note that both axes are in log scale. The number of stars in each panel indicates the significance of the linear interpolation (Pearson test: * $p < 0,05$; ** $p < 0,01$; *** $p < 0,001$). b) Linear correlation coefficient (solid blue lines) between the plastic concentration (y-axis: g km^{-2}, left panel; items/km^2, right panel) and the LPPI for the sites where LPPI ≠ 0, computed by varying the backward advection time τ (x-axis). The solid red lines indicate the *r* of the linear interpolation. Dashed lines indicate the same correlation, but computed by considering all sites. Black dots, when present, indicate that the linear correlation is significant; their size is proportional to the significance of the fit, as indicated in the legend (Pearson test, * $p < 0,05$; ** $p < 0,01$; *** $p < 0,001$). On both panels, the LPPI has been computed with a distance threshold of 0.20°.

nearshore waters. Indeed, according to a numerical model reproducing plastic retention, larger debris are trapped close to the coast due to Stokes drift, while smaller items, less buoyant, are more prone to be transported offshore (Isobe et al., 2014). Larger plastic debris, retained in the coastal waters, are washed up on the beaches, undergoing accelerated degradation (Morales-Caselles et al., 2021) into microplastics and then move progressively offshore. This hypothesis is supported by a significant correlation between coastal source cities (LPPIC index) or rivers (LPPIR index) and areas of high plastic concentration, and by recent work predicting high retention of debris near coastal sources (Baudena et al., 2022; Liubartseva et al., 2018). This indicates that stranding/fragmentation/resuspension is one of the key processes in the dynamics of plastics in the Mediterranean Sea. This may explain the discrepancy between the relatively short lifetime of microplastics in the surface layer and the time required for their aging in the marine environment. Furthermore, the size distribution of plastic debris confirms that the dominant pathway for the formation of secondary MPs is their progressive fragmentation, leading to a gradual increase in the number of fragments to smaller sizes.

The theoretical linear fragmentation model assumes an equal distribution of total volume over the number of size classes, leading to a scaling exponent of 3 (Cózar et al., 2014; Enders et al., 2015). In our study power law regression fitted to particle concentration levels follows a slightly lower exponential $\alpha = 1.6 \pm 0.5$ ($n = 19$), suggesting that fragmentation of plastic in the environment may be partially two-dimensional (Kooi and Koelmans, 2019). Our results for particles >1 mm are consistent with this result, with the prevalence of flat rigid fragment debris showing an exponent of 1.96 (95% confidence interval). As size decreases, a break in slope is observed for particles <1 mm with a smaller increase than expected by continuous fragmentation, probably caused by size-selective removal processes. These results are also confirmed by previous work, and highlight the strong similarities between ocean regions (Cózar et al., 2014, 2017; Reisser et al., 2015). However, the constant supply of particles back and forth from coastal areas may counteract some losses. A discontinuity in the rate of fragmentation has been predicted, when the fragments become very small it tends to a cubic shape fragmenting much faster (Ter Halle et al., 2016). Little is known about the extent to which marine biodegradation contributes to these faster fragmentation rates, as small weight loss (≤ 1%/year) has been found for polyethylene, polypropylene in a laboratory seawater microcosm (Gerritse et al., 2020).

Irregular rigid fragments resulting from the breakdown of larger objects were the most common types of non-fibrous plastics collected in agreement with other studies in Mediterranean (Caldwell et al., 2019; Cózar et al., 2015; Suaria et al., 2016; van der Hal et al., 2017) with higher proportion in the western than eastern basin. Whether detected by ZooScan or by

visual analysis counts, plastic films were found in lower concentrations than fragments even though they represent a significant proportion (37%) of polyolefins (Plastics Europe, 2019). This is likely due to their higher surface-to-volume ratio, which increases biofouling rates compared to other plastics, allowing for faster sinking (Chubarenko et al., 2016). As the separation of categories by ZooScan is based on morphological criteria, improvements are being made to increase the reliability of the analysis.

We showed that the size spectrum of the <1 mm plastic categories differed in their structure. While flat fragments and films showed a flattened curve, Microfibers and filaments were indeed present in surface waters with increasing abundance as size decreased. Although the particle size range in our study (300–1000 μm) is larger than the size range (10–100 μm) studied by Enders et al.(Enders et al., 2015) in the Atlantic Ocean, the slopes display similar behavior. This confirms that fragmentation kinetics are not fully understood and that the intrinsic characteristics of the particles influence their dynamics. For example, settling rates depend on particle surface-to volume ratio, which increases with decreasing particle size upon fragmentation, (Andrady, 2011; Chubarenko et al., 2016; Reisser et al., 2015), as well as on particle shape characteristics such as sphericity and circularity (Van Melkebeke et al., 2020). Biofouling by algae, inclusion in marine snow, ingestion and egestion by zooplankton are biological mechanisms which are likely to affect the fate of plastic debris depending on their characteristics (Cole et al., 2016; Kooi et al., 2017; Kvale et al., 2020). In addition, the density of water particularly high in the case of the Mediterranean may explain that some of the denser particles remain at the surface, as is the case of polyamide contributing to longer residence times and therefore more homogeneous horizontal distributions (Pedrotti et al., 2016). This is the case in our study, although underestimated microfibers are significantly correlated with the presence of polyamide and present throughout the basin. Notably, according to the RCP scenarios adopted by the IPCC, the Mediterranean Sea will become warmer and saltier throughout most of the basin. Our result on the size distribution of the different types of plastics gives us relevant information on their origin and also suggests that the losses of plastics observed for the lower size class may be counterbalanced by the contribution of small fragments from the shoreline.

4.2. Plastic distribution at basin scale

Plastic debris was present at all surface sampling sites in the Mediterranean Sea, confirming widespread contamination throughout the basin. The average plastic abundance (2.60×10^5 km^{-2}) was similar to the single study conducted in 2013 with 30 sites sampled throughout the Mediterranean basin (Cózar et al., 2015) while the average mass concentration is twice as low (423 g km^{-2}), but comparable to the average concentrations measured in the inner accumulation areas of the subtropical oceanic gyres, which ranged from 281 to 639 g/km^2 (Cózar et al., 2014). Our total estimates of surface plastic load, although slightly lower, are consistent with previous estimates based on field surveys (750–3000 metric tons); (Cózar et al., 2015; Ruiz-Orejón et al., 2016; Suaria et al., 2016). This improved estimation based on a large set of data are an order of magnitude lower than those derived from calibration models that estimate 5000–30,000 metric tons, (5%–13% of global mass) and 3–28 trillion particles, (21%–55% of global items) circulation in the basin (Eriksen et al., 2014; Lebreton et al., 2012; van Sebille et al., 2015). These differences are likely related to model constraints, as some key loss processes (sinking, stranding) were not included.

In a recent model, the low plastic loads estimated at the surface (240–390 tons), those being washed ashore (54%) and sinking to the bottom (45%) (Kaandorp et al., 2020), are instead related to the model constraint of low plastic input (4000 tons) compared to previous models that estimated about 100,000 tons (Liubartseva et al., 2018). The latter extrapolated the amount of floating plastic entering the Mediterranean Sea in 2010 from the Jambeck et al. (2015) study by considering that about half of the plastic debris is less dense than sea water. Therefore, there is still debate about these values.

The LPPI allowed us to link the plastic concentration to the history of a water parcel and the magnitude of the land-based plastic sources it encountered in the previous days. The significance is confirmed also when the pollution index was calculated using only cities (LPPIC) or rivers (LPPIR), as well when applying a bootstrap test. These results remain robust within the limits of the variation of distance threshold from terrestrial sources between 0.05 and 0.2°, and the advection period between 5 and 90 days. Beyond this time period the inconsistency between predictions and observations may be due to the difficulty to realistically describe the velocity field i.e., the trajectories of water parcels over a long period of time. This is particularly true while advecting relatively small areas (of the order of the velocity field resolution or less). This may explain also why several locations presented a LPPI value equal to zero: the advection time may have not been long enough for the plastic debris to reach its source. In addition, plastic debris is affected by dynamics other than physical transport, such as biofouling, beaching, washing-off, fragmentation, etc. which were not considered. For instance, plastic debris may be generated from break of larger items in a location far from their source. However, on the other hand, the short time scale (a few weeks) obtained agrees with the average residence time of plastics in the Mediterranean Sea reported in previous studies (Baudena et al., 2022; Liubartseva et al., 2018). Overall, the LPPI, despite these limitations, seems a promising diagnostic to predict plastic concentration. Indeed, it has the advantage of needing a single backward advection of a water parcel in order to estimate its plastic content. Classical plastic-tracking models need to perform a simulation over the entire basin and possibly over multiple years, which is both complex, time consuming and computationally expensive.

Although field data converge on the occurrence of relatively small loads compared to expected inflows, they should be supported by a better assessment of leakage mechanisms. For example, in the Mediterranean, the PP/PE ratio tends to increase as size decreases, which may indicate faster degradation of PP that sediment or fragment more rapidly (Kedzierski et al., 2022). If this ratio is much lower than riverine (and other) inputs and the estimated mean residence time is low, it is possible that most PP microplastics are at the bottom of the Mediterranean Sea. Reliable data on the environmental pathways of plastic waste would allow for a better estimate of global inputs, as shown by Weiss et al. (Weiss et al., 2021), who obtained estimates that were two to three orders of magnitude lower than currently estimated riverine fluxes.

4.3. Plastic distribution at a regional scale on the surface of the Mediterranean Sea

During the Tara Mediterranean expedition, we sampled floating plastic in most of the Mediterranean basins from Gibraltar to Lebanon. Our results show that the distribution of plastic debris in terms of abundance, mass and size at the surface of the Mediterranean Sea is uneven and marked by regional differences with areas of very high abundance, such as Cape Corsica, and very low abundance, such as the inner part of the Levantine basin reflecting the high temporal and spatial variability of the currents (Fig. 1).

4.3.1. Western Mediterranean Sea

Although few measurements have been made, a great variability of concentrations in abundance and weight of plastic has been observed in the Alboran Sea and near Gibraltar. This was likely due to differences in plastic input induced by the mesoscale circulation associated with Atlantic Water (AW) inflow (Millot and Taupier-Letage, 2005). It has been suggested that some of the floating plastic pollution in the Mediterranean originates from outside the basin (Cózar et al., 2015). The AW form the Algerian Current (AC) which flows along the African coast, the concentrations of plastic found are not homogeneous, it may be inputs from large cities such as Algiers or Bizerte because few rivers have their confluences on these coasts and the construction of dams reduces the flow of rivers to the sea and traps sediments in the reservoirs of the dams, including plastics from the catchments.

Tyrrhenian Basin: near the Sicily Strait level, the light surface AW divides into two branches. The first one is directed northwards entering the Tyrrhenian Sea flowing along the Italian coasts creating the Northern Current (NC). The Tyrrhenian Basin, although not statistically different, had the highest average concentrations of plastic debris, which can be explained by its presence in large quantities near northern Sicily and in the Gulf of Naples. In addition, the relatively lower number-to-mass ratio and a high surface area occupied by plastics (1463 m2 km^{-2}), suggest that particles were less aged in this area than in other regions, indicating the existence of local sources of microplastic pollution. This is also corroborated by a significantly lower proportion of poly(ethylene) (PE) than the average value for the Mediterranean Sea (57.9 ± 10.5%), (Kedzierski et al., 2022) results interpreted as the possible signal of nearby plastic sources. Another source that could be added to explain this high contamination is the maritime activity in the Tyrrhenian Sea; more locally, in the strait of Bonifacio, a model-derived estimate that sea-based litter has been shown to account for 87% of total litter, as a consequence of shipping routes and leisure boating (Liubartseva et al., 2019). Plastic debris, pushed by currents and winds, reaches the Strait of Corsica where the highest abundance of plastic was observed in our study (up to 8 million items km^{-2}). The Corsica Channel in the border between the Tyrrhenian Sea and the Ligurian Sea was also identified as a plastic hotspot by other studies (Caldwell et al., 2019; Suaria et al., 2016). While not a true accumulation area, the high level of contamination is likely induced by seasonal circulation, particularly during summer when the East Corsican Current is less intense than in winter (Fossi et al., 2017; Mansui et al., 2015). Furthermore, a recent study on plastic debris tracking in the Mediterranean, where the slope of the coastline was incorporated into the model, showed that the effect of stranding is regulated by the length and topography of the coastline. When currents are directed towards Cape Corsica, plastic debris accumulates there because the steepness of the local shoreline prevents it from being beached (Baudena et al., 2022).

The Ligurian-Provençal and Balearic Sea: Corsica Channel is one of the entrances to the Pelagos Sanctuary, a marine protected area (MPA), where fin whales are exposed to microplastic ingestion during the summer feeding season (Fossi et al., 2012). In this region, where the NC flows cyclonically along the continental slope of the Ligurian-Provençal sub-basin (Millot and Taupier-Letage, 2005) we observed high concentrations of plastic especially between Nice and Toulon ($> 5 \times 10^5$ items km^{-2}). The Ligurian Sea has also been identified by other authors (Collignon et al., 2012; Pedrotti et al., 2016) as having a plastic concentration about seven times higher than that of the Sardinian Sea in the southern direction (average value of 0.13 items m^{-3}) (de Lucia et al., 2014). Further east in the Gulf of Lion, in the bay of Marseille, the average abundance of plastic (1.2×10^5 items km^{-2}) is similar to that observed over the same period (1.1 10^5 items km^{-2}) by Schmidt et al. (2018) whereas the average weight observed is 5 times greater in our study. This suggests that large cities like Marseille and the rivers like Rhone are sources of plastics displaying very short scale variability. Indeed, Ourmieres et al. (Ourmieres et al., 2018) showed that on the French Riviera, the winds and the NC drive the stranding or the transport of floating plastic debris either by forming a cross-shore transport barrier, keeping them close to the coast as in our results, or by exporting them offshore. The main branch of the NC continues along the Balearic Sea, considered one of the most plastic-polluted areas in the Mediterranean (de Haan et al., 2019). In our sampling stations, 89% of the plastic mass collected was composed of macroplastics, which corroborates that this area is probably a source of plastics from large cities like Barcelona or adjacent rivers (González-Fernández et al., 2021). Plastic debris was also detected in the Sardinian Sea in greater quantities than in other studies (Ruiz-Orejón et al., 2016). This could be attributed to the confluence of the Balearic Current (BC) associated with the Stokes drift, which tends to reinforce the plastic transport from the densely populated areas of the southeastern Gulf of Lions to the north African coast (Liubartseva et al., 2018; Millot and Taupier-Letage, 2005).

4.3.2. The Eastern Mediterranean Sea

The second branch of AW turns southward, entering the eastern basin through the Strait of Sicily forming the Libyan Current (Millot and Taupier-Letage, 2005). Towards the central Ionian Sea, we observed significant concentrations of plastics, although this area is considered a diffusive zone with relatively moderate predictions of plastic debris (~5–7 g km^{-2}), (Liubartseva et al., 2018). One explanation is their marine origin via the Atlantic Ionian Stream (AIS) where shipping lanes are particularly dense in this area. This hypothesis is supported by the unstable nature of the Libyan current, which locally generates a series of cyclonic and anticyclonic gyres preventing the transport of plastics towards the center of the basin (Sorgente et al., 2011). The only field study in the Tunisian shelf/Gulf of Sidra showed that surface waters in the Gulf of Gabes have low concentrations of plastics (Zayen et al., 2020) supporting models that predict that in the south, the Libyan coastline is not exposed to high inputs of terrestrial litter (<2 g km^{-2}).

The strong Lybian-Egyptian current flows into the Levantine Sea towards the eastern end of the basin, then turns sharply northward, spreading along the coast to arrive near the Turkish coast. From Israel to Lebanon high concentrations of plastic have been found (van der Hal et al., 2017). These coastal areas are potential sinks for plastics (Duncan et al., 2018) but also sources as plastic debris can be transported north along the Turkish coast (Gündoğdu and Çevik, 2017). Turkish coasts are also receptors of plastic from adjacent rivers, which explains the high concentration and expected high flux of plastic especially in Mersin Bay (Gündoğdu et al., 2018; Lebreton et al., 2017). As mentioned above, we were not able to sample the coastal areas of the Levantine Basin, our sampling stations are located inland near and off the coast of Cyprus. Our results reflect an open sea condition and do not account for the high plastic load observed in these coastal areas. These patterns do not match the accumulation areas predicted by global particle tracking models due to the imprecise resolution of the mesoscale field in the sub-basin (van Sebille et al., 2015), and the very high levels measured (van der Hal et al., 2017), but agree with models that, by including stranding and sedimentation rates, predict retention areas near the shoreline (Baudena et al., 2022; Liubartseva et al., 2018; Soto-Navarro et al., 2020). Indeed, the abundance and mass concentration of plastics are the lowest found in the entire Mediterranean and the size distribution of plastics differs significantly from the other sub-basins, suggesting that the plastics are isolated with probable decoupling from the sources. The observed results are likely related to the complexity of the large cyclonic circulation in this NE Levantine basin (Estournel et al., 2021). In the northern part, the counterclockwise wind and the barrier effect of the Mediterranean current limit exchanges with open areas, favoring the flow of plastic debris along the shoreline (Gündoğdu et al., 2018). In the southern part, the transport of plastics from the Egyptian coast to the inner part of the basin appears to be suppressed by an intense, shore-directed, Stokes drift (Liubartseva et al., 2018). Backward analysis of particle drift on Cyprus beaches shows that most plastics likely originated in the basin (Duncan et al., 2018). This is supported by a high rate of PE observed in the eastern basin (Kedzierski et al., 2022). We hypothesize that the debris that can escape the Stokes drift is likely trapped in the larger system of Cyprus persistent anticyclonic eddies (Estournel et al., 2021). By isolating plastics from coastal sources, a segregation phenomenon occurred; thus, denser polymers (e.g., PA, boat paints) would tend to sediment and their percentages would decrease rapidly (Kedzierski et al., 2022).

This pattern of plastic dynamics was observed in the summer (August 2–19) in the low runoff season and can vary significantly during the winter period when runoff plays an important role in plastic transport from freshwater systems (Lebreton et al., 2017). Flooding periods along the Turkish coast, resulted in a significant increase in plastic concentrations and a decrease in PE rates; in Mersin Bay the average particle size also dropped in the sampling from 2.37 mm to 1.13 mm before and after the floods events (Gündoğdu et al., 2018). Other scenarios of circulation and accumulation of floating litter also predicted an eastward and shoreward shift in winter (Macias et al., 2019).

Further out in the Aegean Sea, several eddies are found around the island of Crete and the Greek coast, while the dominant currents flowing towards the Ionian Sea where they are redirected southward along the eastern coasts of Sicily (Millot and Taupier-Letage, 2005). Concentrations of plastic debris between Cyprus and Crete were low (Fig. 1), in agreement

with models that predict a zone of plastic dispersal from the Asia Minor Current to the southern Aegean Sea (Baudena et al., 2022; Liubartseva et al., 2018; Macias et al., 2019; Soto-Navarro et al., 2020). With the exception of a hotspot area in the Saronic Gulf (Greece), likely related to inputs from the Athens metropolitan area and in agreement with other studies (Adamopoulou et al., 2021; Ruiz-Orejón et al., 2016), low concentrations of plastics have been detected between the islands in the center of the sub-basin (average $8 \times 10^4\,km^{-2}$). This corresponds to a predicted less polluted area, probably due to the filtering effect of the numerous islands and a remote plastic source (Politikos et al., 2017). Another area of high plastic concentration was found in the Gulf of Taranto, in the northern Ionian Sea. This is a complex area also polluted by organic or inorganic contaminants where anthropogenic factors seem to be the most important pollution sources (Cotecchia et al., 2021).

The Tara Mediterranean expedition allowed us to undertake an integrative study with a large amount of new data and parameters on plastic never collected before. Examination of the distribution of floating plastic debris in the different sub-basins show lower concentrations of plastics in the Levantine and Aegean basins and although not significantly different, the Tyrrhenian basin shows a characteristic distribution with a high accumulation in its northern part. The spatial resolution of the data allowed us to target areas of high plastic concentration and, using LPPI, to link the plastic concentration to the water mass and land sources encountered. Use of this tool could help prioritize mitigation strategies and facilitate future predictions as it can provide a means to estimate plastic concentrations.

According to our results hundreds of billions of plastic debris float on the surface of the Mediterranean of which 95% are <5 mm. Therefore, our results reflect the lower limit of the surface plastic pollution carried out mainly during low runoff seasons. Additional sampling is needed during the high runoff winter period to account for climate change, flooding and shoreline erosion.

Our study demonstrated the importance of acquiring and analyzing a series of parameters for each object such as size, surface area, weight, grade, etc. Using imaging methods, we obtained a comprehensive and standardized database of ~75,000 plastics which, coupled with their chemical characterization (Kedzierski et al., 2019b, 2022) provide us with a unique dataset that can be used for later investigations. These results allowed us to obtain reliable estimates of plastic dynamics and to identify the advanced state of plastic degradation that supports the hypothesis of multiple stranding and resuspension of plastic particles. This may indicate that the processes leading to the formation of microplastics in the Mediterranean were mainly initiated on land or in rivers.

Monitoring changes in plastic morphological parameters is an important step in understanding the fate of plastics in the oceans and should be combined with quantitative land-sea assessments and the tracking of atmospheric deposition. Nano- and microplastic can be released from the marine environment into the atmosphere by sea-sprays (Trainic et al., 2020).

Although some plastic variables in our study correlate with patterns of ocean productivity, they are likely to be more related to water mass circulation than to biological activity. We still lack the knowledge to predict with certainty at what level the presence of plastics might affect the resilience of marine ecosystems. A recent modeling study showed that consumption of microplastics by zooplankton can reduce grazing pressure on primary producers with biogeochemical consequences depending on the trophic status of the system (Kvale et al., 2021).

Because the vast majority of plastics observed are small, it is nearly impossible to actively remove those that have already accumulated in the environment, leading us to believe that the primary solutions for mitigating this pollution lie on land. All in all, only an integrative approach to transforming the global plastics economy can provide solutions for better waste management and reduced future plastic emissions (Borrelle et al., 2020).

CRediT authorship contribution statement

M.L.P., R.T., G.G. participated in the design and coordination of field surveys.

M.L.P., F.G., A.E., S.P., M.H., E.B. collected the samples.

A.E., S.P., M.H. performed laboratory work.

M.L.P., F.L., A.B., G.R, E.S-G. M.K., E.B. analyzed the data,

M.L.P., A.B. wrote the manuscript and all authors reviewed and edited the manuscript.

Funding

The Tara Ocean Foundation acknowledges the commitment of the following sponsors its founders: CNRS, Sorbonne University, LOV, Genoscope/CEA, agnès b., Etienne Bourgois, the Veolia Environment Foundation, Lorient Agglomeration, Serge Ferrari, the Foundation Prince Albert II de Monaco, IDEC. This work was supported by the Institute of Ecology and Environment of the CNRS (INEE) grant, the French Ministry of Environment (MTES). Part of this work was performed within the EU Marine Strategy Framework Directive (MSFD).

Declaration of competing interest

The authors declare that they have no known competing financial interests or personal relationships that could have appeared to influence the work reported in this paper.

Acknowledgments

We thank the Tara" schooner, crews and the teams that helped with the collection of samples during the cruise. The authors are grateful to Marie-Emmanuelle Kerros, Gerasimos Korres, Juliette Mauri, Lisa Rouaud-Clergues, Maxime Olsommer for their help in samples analysis. We thank MERCATOR-CORIOLIS and ACRI-ST for providing daily satellite data during the expedition and Copernicus Marine Environment Monitoring Service (CMEMS, http://marine.copernicus.eu/). We are also grateful to the French Ministry of Foreign Affairs for supporting the expedition and to the countries that granted sampling permission.

Appendix A. Supplementary data

Supplementary data to this article can be found online at https://doi.org/10.1016/j.scitotenv.2022.155958.

References

Adamopoulou, A., Zeri, C., Garaventa, F., Gambardella, C., Ioakeimidis, C., Pitta, E., 2021. Distribution patterns of floating microplastics in open and coastal waters of the eastern Mediterranean Sea (Ionian, Aegean, and Levantine Seas). Front. Mar. Sci. 8, 1–15. https://doi.org/10.3389/fmars.2021.699000.

Andrady, A.L., 2011. Microplastics in the marine environment. Mar. Pollut. Bull. 62, 1596–1605. https://doi.org/10.1016/j.marpolbul.2011.05.030.

Barrows, A.P.W., Cathey, S.E., Petersen, C.W., 2018. Marine environment microfiber contamination: global patterns and the diversity of microparticle origins. Environ. Pollut. 237, 275–284. https://doi.org/10.1016/j.envpol.2018.02.062.

Baudena, A., Ser-Giacomi, E., D'Onofrio, D., Capet, X., Cotté, C., Cherel, Y., D'Ovidio, F., 2021. Fine-scale structures as spots of increased fish concentration in the open ocean. Sci. Rep. 11, 1–13. https://doi.org/10.1038/s41598-021-94368-1.

Baudena, A., Ser-Giacomi, E., Jalon-Rojas, I., Galgani, F., Pedrotti, M.L., 2022. The streaming of plastic in the Mediterranean Sea. Nat. Commun. https://doi.org/10.1038/s41467-022-30572-5.

Borrelle, S.B., Ringma, J., Lavender Law, K., Monnahan, C.C., Lebreton, L., McGivern, A., Murphy, E., Jambeck, J., Leonard, G.H., Hilleary, M.A., Eriksen, M., Possingham, H.P., De Frond, H., Gerber, L.R., Polidoro, B., Tahir, A., Bernard, M., Mallos, N., Barnes, M., Rochman, C.M., 2020. Predicted growth in plastic waste exceeds efforts to mitigate plastic pollution. Science (80-.) 369, 1515–1518. https://doi.org/10.1126/SCIENCE.ABA3656.

Boss, E., Picheral, M., Leeuw, T., Chase, A., Karsenti, E., Gorsky, G., Taylor, L., Slade, W., Ras, J., Claustre, H., 2013. The characteristics of particulate absorption, scattering and attenuation coefficients in the surface ocean; contribution of the Tara Oceans expedition. Methods Oceanogr. 7, 52–62. https://doi.org/10.1016/j.mio.2013.11.002.

Caldwell, J., Petri-Fink, A., Rothen-Rutishauser, B., Lehner, R., 2019. Assessing meso- and microplastic pollution in the Ligurian and Tyrrhenian seas. Mar. Pollut. Bull. 149, 110572. https://doi.org/10.1016/j.marpolbul.2019.110572.

Chubarenko, I., Bagaev, A., Zobkov, M., Esiukova, E., 2016. On some physical and dynamical properties of microplastic particles in marine environment. Mar. Pollut. Bull. 108, 105–112. https://doi.org/10.1016/j.marpolbul.2016.04.048.

Cole, M., Lindeque, P.K., Fileman, E., Clark, J., Lewis, C., Halsband, C., Galloway, T.S., 2016. Microplastics alter the properties and sinking rates of zooplankton faecal pellets. Environ. Sci. Technol. 50, 3239–3246. https://doi.org/10.1021/acs.est.5b05905.

Collignon, A., Hecq, J.H., Glagani, F., Voisin, P., Collard, F., Goffart, A., 2012. Neustonic microplastic and zooplankton in the North Western Mediterranean Sea. Mar. Pollut. Bull. 64, 861–864. https://doi.org/10.1016/j.marpolbul.2012.01.011.

Cotecchia, F., Vitone, C., Sollecito, F., Miccoli, D., Petti, R., Milella, D., 2021. OPEN a geo-chemo-mechanical study of a highly polluted marine system (Taranto, Italy) for the enhancement of the conceptual site model. Sci. Rep. 1–26. https://doi.org/10.1038/s41598-021-82879-w.

Cózar, A., Echevarría, F., González-Gordillo, J.I., Irigoien, X., Úbeda, B., Hernández-León, S., Palma, Á.T., Navarro, S., García-de-Lomas, J., Ruiz, A., Fernández-de-Puelles, M.L., Duarte, C.M., 2014. Plastic debris in the open ocean. Proc. Natl. Acad. Sci. U. S. A. 111, 10239–10244. https://doi.org/10.1073/pnas.1314705111.

Cózar, A., Sanz-Martín, M., Martí, E., González-Gordillo, J.I., Ubeda, B., Á.Gálvez, J., Irigoien, X., Duarte, C.M., 2015. Plastic accumulation in the Mediterranean sea. PLoS One 10, 1–12. https://doi.org/10.1371/journal.pone.0121762.

Cózar, A., Martí, E., Duarte, C.M., García-de-Lomas, J., Van Sebille, E., Ballatore, T.J., Eguíluz, V.M., Ignacio González-Gordillo, J., Pedrotti, M.L., Echevarría, F., Troublè, R., Irigoien, X., 2017. The Arctic Ocean as a dead end for floating plastics in the North Atlantic branch of the Thermohaline Circulation. Sci. Adv. 3. https://doi.org/10.1126/sciadv.1600582.

Declaration, B., 1995. Declaration, Barcelona. Adopted at the Euro-Mediterranean Conference, 27-28 November 1995. European Commission, Brussels 1995.

Duncan, E.M., Arrowsmith, J., Bain, C., Broderick, A.C., Lee, J., Metcalfe, K., Pikesley, S.K., Snape, R.T.E., van Sebille, E., Godley, B.J., 2018. The true depth of the Mediterranean plastic problem: extreme microplastic pollution on marine turtle nesting beaches in Cyprus. Mar. Pollut. Bull. 136, 334–340. https://doi.org/10.1016/j.marpolbul.2018.09.019.

Enders, K., Lenz, R., Stedmon, C.A., Nielsen, T.G., 2015. Abundance, size and polymer composition of marine microplastics ≥10 μm in the Atlantic Ocean and their modelled vertical distribution. Mar. Pollut. Bull. 100, 70–81. https://doi.org/10.1016/j.marpolbul.2015.09.027.

Enders, K., Lenz, R., Ivar do Sul, J.A., Tagg, A.S., Labrenz, M., 2020. When every particle matters: a QuEChERS approach to extract microplastics from environmental samples. MethodsX 7, 100784. https://doi.org/10.1016/j.mex.2020.100784.

Eriksen, M., Lebreton, L.C.M., Carson, H.S., Thiel, M., Moore, C.J., Borerro, J.C., Galgani, F., Ryan, P.G., Reisser, J., 2014. Plastic pollution in the world's oceans: more than 5 trillion plastic pieces weighing over 250,000 tons afloat at sea. PLoS One 9, 1–15. https://doi.org/10.1371/journal.pone.0111913.

Estournel, C., Marsaleix, P., Ulses, C., 2021. A new assessment of the circulation of Atlantic and intermediate waters in the Eastern Mediterranean. Prog. Oceanogr. 198, 102673. https://doi.org/10.1016/j.pocean.2021.102673.

Fazey, F.M.C., Ryan, P.G., 2016. Debris size and buoyancy influence the dispersal distance of stranded litter. Mar. Pollut. Bull. 110, 371–377. https://doi.org/10.1016/j.marpolbul.2016.06.039.

Fossi, M.C., Panti, C., Guerranti, C., Coppola, D., Giannetti, M., Marsili, L., Minutoli, R., 2012. Are baleen whales exposed to the threat of microplastics? A case study of the Mediterranean fin whale (Balaenoptera physalus). Mar. Pollut. Bull. 64, 2374–2379. https://doi.org/10.1016/j.marpolbul.2012.08.013.

Fossi, M.C., Romeo, T., Baini, M., Panti, C., Marsili, L., Campan, T., Canese, S., Galgani, F., Druon, J.N., Airoldi, S., Taddei, S., Fattorini, M., Brandini, C., Lapucci, C., 2017. Plastic debris occurrence, convergence areas and fin whales feeding ground in the Mediterranean marine protected area Pelagos Sanctuary: a modeling approach. Front. Mar. Sci. 4, 1–15. https://doi.org/10.3389/fmars.2017.00167.

Galgani, F., Hanke, G., Werner, S., De Vrees, L., 2013. Marine litter within the European Marine Strategy Framework Directive. ICES J. Mar. Sci. 70, 1055–1064. https://doi.org/10.1093/icesjms/fst122.

Gerritse, J., Leslie, H.A., Tender, C.A.De, Devriese, L.I., Vethaak, A.D., 2020. Fragmentation of plastic objects in a laboratory seawater microcosm. Sci. Rep. 1–16. https://doi.org/10.1038/s41598-020-67927-1.

Gilfillan, L.R., Ohman, M.D., Doyle, M.J., Watson, W., 2009. Occurrence of plastic microdebris in the southern California Current system. Calif. Coop. Ocean. Fish. Investig. Reports. 50, pp. 123–133.

Goldstein, M.C., Titmus, A.J., Ford, M., 2013. Scales of spatial heterogeneity of plastic marine debris in the northeast Pacific Ocean. PLoS One 8. https://doi.org/10.1371/journal.pone.0080020.

González-Fernández, D., Cózar, A., Hanke, G., Viejo, J., Morales-Caselles, C., Bakiu, R., Barceló, D., Bessa, F., Bruge, A., Cabrera, M., Castro-Jiménez, J., Constant, M., Crosti, R., Galletti, Y., Kideys, A.E., Machitadze, N., Pereira de Brito, J., Pogojeva, M., Ratola, N., Rigueira, J., Rojo-Nieto, E., Savenko, O., Schöneich-Argent, R.I., Siedlewicz, G., Suaria, G., Tourgeli, M., 2021. Floating macrolitter leaked from Europe into the ocean. Nat. Sustain. 4, 474–483. https://doi.org/10.1038/s41893-021-00722-6.

Gorsky, G., Ohman, M.D., Picheral, M., Gasparini, S., Stemmann, L., Romagnan, J.B., Cawood, A., Pesant, S., García-Comas, C., Prejger, F., 2010. Digital zooplankton image analysis using the ZooScan integrated system. J. Plankton Res. 32, 285–303. https://doi.org/10.1093/plankt/fbp124.

Gündoğdu, S., Çevik, C., 2017. Micro- and mesoplastics in Northeast Levantine coast of Turkey: the preliminary results from surface samples. Mar. Pollut. Bull. 118, 341–347. https://doi.org/10.1016/j.marpolbul.2017.03.002.

Gündoğdu, S., Çevik, C., Ayat, B., Aydoğan, B., Karaca, S., 2018. How microplastics quantities increase with flood events? An example from Mersin Bay NE Levantine coast of Turkey. Environ. Pollut. 239, 342–350. https://doi.org/10.1016/j.envpol.2018.04.042.

de Haan, W.P., Sanchez-Vidal, A., Canals, M., 2019. Floating microplastics and aggregate formation in the Western Mediterranean Sea. Mar. Pollut. Bull. 140, 523–535. https://doi.org/10.1016/j.marpolbul.2019.01.053.

van der Hal, N., Ariel, A., Angel, D.L., 2017. Exceptionally high abundances of microplastics in the oligotrophic Israeli Mediterranean coastal waters. Mar. Pollut. Bull. 116, 151–155. https://doi.org/10.1016/j.marpolbul.2016.12.052.

Hanke, G., Galgani, F., Werner, S., Oosterbaan, L., Nilsson, P., Fleet, D., Kinsey, S., Thompson, R., Van Franeker, J., Vlachogianni, T., Palatinus, A., Scoullos, M., Veiga, J., Matiddi, M., Alcaro, L., Maes, T., Korpinen, S., Budziak, A., Leslie, H., Gago, J., Liebezeit, G., 2013. Guidance on Monitoring of Marine Litter in European Seas. https://doi.org/10.2788/99475.

Hidalgo-ruz, V., Gutow, L., Thompson, R.C., Thiel, M., 2012. Microplastics in the marine environment: a review of the methods used for identification and quantification. Environ. Sci. Technol. 46, 3060–3075. https://doi.org/10.1021/es2031505.

Hidalgo-Ruz, V., Honorato-Zimmer, D., Gatta-Rosemary, M., Nuñez, P., Hinojosa, I.A., Thiel, M., 2018. Spatio-temporal variation of anthropogenic marine debris on Chilean beaches. Mar. Pollut. Bull. 126, 516–524. https://doi.org/10.1016/j.marpolbul.2017.11.014.

Isobe, A., Kubo, K., Tamura, Y., Kako, S., Nakashima, E., Fujii, N., 2014. Selective transport of microplastics and mesoplastics by drifting in coastal waters. Mar. Pollut. Bull. 89, 324–330. https://doi.org/10.1016/j.marpolbul.2014.09.041.

Isobe, A., Azuma, T., Cordova, M.R., Cózar, A., Galgani, F., Hagita, R., Kanhai, L.D., Imai, K., Iwasaki, S., Kako, S., Kozlovskii, N., Lusher, A.L., Mason, S.A., Michida, Y., Mituhasi, T., Morii, Y., Mukai, T., Popova, A., Shimizu, K., Tokai, T., Uchida, K., Yagi, M., Zhang, W., 2021. A multilevel dataset of microplastic abundance in the world's upper ocean and the Laurentian Great Lakes. Microplast.Nanoplast.s 1, 1–14. https://doi.org/10.1186/s43591-021-00013-z.

Jahnke, A., Arp, H.P.H., Escher, B.I., Gewert, B., Gorokhova, E., Kühnel, D., Ogonowski, M., Potthoff, A., Rummel, C., Schmitt-Jansen, M., Toorman, E., MacLeod, M., 2017. Reducing uncertainty and confronting ignorance about the possible impacts of weathering plastic in the marine environment. Environ. Sci. Technol. Lett. 4, 85–90. https://doi.org/10.1021/acs.estlett.7b00008.

Jambeck, J.R., Geyer, R., Wilcox, C., Siegler, T.R., Perryman, M., Andrady, A., Narayan, R., Law, K.L., 2015. Plastic waste inputs from land into the ocean in 2010. Science (80-.) 347, 768–771. https://doi.org/10.1126/science.1260352.

Kaandorp, M.L.A., Dijkstra, H.A., Sebille, E.Van, 2020. Closing the Mediterranean Marine Floating Plastic Mass Budget: Inverse Modeling of Sources And Sinks. https://doi.org/10.1021/acs.est.0c01984.

Kato, M., Asokan, V.A., Devaporihartakula, C., Inoue, M., Aoki-Suzuki, C., Fushimi, E., Hotta, Y., 2021. G20 Report on Actions Against Marine Plastic Litter: Third Information Sharing Based on the G20 Implementation Framework.

Kedzierski, M., Falcou-Préfol, M., Kerros, M.E., Henry, M., Pedrotti, M.L., Bruzaud, S., 2019a. A machine learning algorithm for high throughput identification of FTIR spectra: application on microplastics collected in the Mediterranean Sea. Chemosphere 234. https://doi.org/10.1016/j.chemosphere.2019.05.113.

Kedzierski, M., Villain, J., Falcou-Préfol, M., Kerros, M.E., Henry, M., Pedrotti, M.L., Bruzaud, S., 2019b. Microplastics in Mediterranean Sea: a protocol to robustly assess contamination characteristics. PLoS One 14. https://doi.org/10.1371/journal.pone.0212088.

Kedzierski, M., Palazot, M., Soccalingame, L., Falcou-Préfol, M., Gorsky, G., Galgani, F., Bruzaud, S., Pedrotti, M.L., 2022. Chemical composition of microplastics floating on the surface of the Mediterranean Sea. Mar. Pollut. Bull. 174. https://doi.org/10.1016/j.marpolbul.2021.113284.

Kershaw, P., Turra, P., Galgani, F., 2019. Guidelines for the Monitoring And Assessment of Plastic Litter in the Ocean: GESAMP Joint Group of Experts on the Scientific Aspects of Marine Environmental Protection. Rep. Stud. GESAMP no 99. 138.

Kooi, M., Koelmans, A.A., 2019. Simplifying Microplastic Via Continuous Probability Distributions for Size, Shape, And Density. https://doi.org/10.1021/acs.estlett.9b00379.

Kooi, M., Van Nes, E.H., Scheffer, M., Koelmans, A.A., 2017. Ups and downs in the ocean: effects of biofouling on vertical transport of microplastics. Environ. Sci. Technol. 51, 7963–7971. https://doi.org/10.1021/acs.est.6b04702.

Kukulka, T., Proskurowski, G., Morét-Ferguson, S., Meyer, D.W., Law, K.L., 2012. The effect of wind mixing on the vertical distribution of buoyant plastic debris. Geophys. Res. Lett. 39, 1–6. https://doi.org/10.1029/2012GL051116.

Kvale, K., Prowe, A.E.F., Chien, C.T., Landolfi, A., Oschlies, A., 2020. The global biological microplastic particle sink. Sci. Rep. 10, 1–12. https://doi.org/10.1038/s41598-020-72898-4.

Kvale, K., Prowe, A.E.F., Chien, C.T., Landolfi, A., Oschlies, A., 2021. Zooplankton grazing of microplastic can accelerate global loss of ocean oxygen. Nat. Commun. 12. https://doi.org/10.1038/s41467-021-22554-w.

Lebreton, L.C.M., Greer, S.D., Borrero, J.C., 2012. Numerical modelling of floating debris in the world's oceans. Mar. Pollut. Bull. 64, 653–661. https://doi.org/10.1016/j.marpolbul.2011.10.027.

Lebreton, L., Zwet, J., Damsteg, J., Slat, B., Andrady, A., Reisser, J., 2017. River plastic emissions to the world's oceans. Nat. Commun. 8. https://doi.org/10.1038/ncomms15611.

Lebreton, L., Egger, M., Slat, B., 2019. A global mass budget for positively buoyant macroplastic debris in the ocean. Sci. Rep. 9, 1–10. https://doi.org/10.1038/s41598-019-49413-5.

Li, W.C., Tse, H.F., Fok, L., 2016. Plastic waste in the marine environment: a review of sources, occurrence and effects. Sci. Total Environ. 566–567, 333–349. https://doi.org/10.1016/j.scitotenv.2016.05.084.

Liubartseva, S., Coppini, G., Lecci, R., Clementi, E., 2018. Tracking plastics in the Mediterranean: 2D Lagrangian model. Mar. Pollut. Bull. 129, 151–162. https://doi.org/10.1016/j.marpolbul.2018.02.019.

Liubartseva, S., Coppini, G., Lecci, R., 2019. Model-based identification of marine plastic sources for the Mediterranean Marine Protected Areas ! 2019–2020.

Llorca, M., Álvarez-muñoz, D., Ábalos, M., Rodríguez-mozaz, S., Santos, L.H.M.L.M., León, V.M., Campillo, J.A., Martínez-gómez, C., Abad, E., Farré, M., 2020. Trends in environmental analytical chemistry microplastics in Mediterranean coastal area: toxicity and impact for the environment and human health. Biochem. Pharmacol. 27, e00090. https://doi.org/10.1016/j.teac.2020.e00090.

de Lucia, G.A., Caliani, I., Marra, S., Camedda, A., Coppa, S., Alcaro, L., Campani, T., Giannetti, M., Coppola, D., Cicero, A.M., Panti, C., Baini, M., Guerranti, C., Marsili, L., Massaro, G., Fossi, M.C., Matiddi, M., 2014. Amount and distribution of neustonic micro-plastic off the western Sardinian coast (Central-Western Mediterranean Sea). Mar. Environ. Res. 100, 10–16. https://doi.org/10.1016/j.marenvres.2014.03.017.

Lusher, A.L., Tirelli, V., O'Connor, I., Officer, R., 2015. Microplastics in Arctic polar waters: the first reported values of particles in surface and sub-surface samples. Sci. Rep. 5, 1–9. https://doi.org/10.1038/srep14947.

Macias, D., Cózar, A., Garcia-gorriz, E., González-fernández, D., Stips, A., 2019. Surface water circulation develops seasonally changing patterns of fl oating litter accumulation in the Mediterranean Sea.A modelling approach. Mar. Pollut. Bull. 149, 110619. https://doi.org/10.1016/j.marpolbul.2019.110619.

Mansui, J., Molcard, A., Ourmières, Y., 2015. Modelling the transport and accumulation of floating marine debris in the Mediterranean basin. Mar. Pollut. Bull. 91, 249–257. https://doi.org/10.1016/j.marpolbul.2014.11.037.

Millot, C., Taupier-Letage, I., 2005. Circulation in the Mediterranean Sea. 5, pp. 29–66. https://doi.org/10.1007/b107143.

Morales-Caselles, C., Viejo, J., Martí, E., González-Fernández, D., Pragnell-Raasch, H., González-Gordillo, J.I., Montero, E., Arroyo, G.M., Hanke, G., Salvo, V.S., Basurko, O.C., Mallos, N., Lebreton, L., Echevarría, F., van Emmerik, T., Duarte, C.M., Gálvez, J.A., van Sebille, E., Galgani, F., García, C.M., Ross, P.S., Bartual, A., Ioakeimidis, C., Markalain, G., Isobe, A., Cózar, A., 2021. An inshore–offshore sorting system revealed from global classification of ocean litter. Nat. Sustain. 4, 484–493. https://doi.org/10.1038/s41893-021-00720-8.

Morét-Ferguson, S., Law, K.L., Proskurowski, G., Murphy, E.K., Peacock, E.E., Reddy, C.M., 2010. The size, mass, and composition of plastic debris in the western North Atlantic Ocean. Mar. Pollut. Bull. 60, 1873–1878. https://doi.org/10.1016/j.marpolbul.2010.07.020.

Ourmieres, Y., Mansui, J., Molcard, A., Galgani, F., Poitou, I., 2018. The boundary current role on the transport and stranding of floating marine litter: the French Riviera case. Cont. Shelf Res. 155, 11–20. https://doi.org/10.1016/j.csr.2018.01.010.

Pabortsava, K., Lampitt, R.S., 2020. High concentrations of plastic hidden beneath the surface of the Atlantic Ocean. Nat. Commun. 11, 1–11. https://doi.org/10.1038/s41467-020-17932-9.

Paper, C., Suaria, G., National, I., Aliani, S., National, I., Suaria, G., 2016. Abundance, distribution and composition of floating debris in the Mediterranean Sea. https://doi.org/10.13140/RG.2.1.3101.8086.

Pedrotti, M.L., Petit, S., Elineau, A., Bruzaud, S., Crebassa, J.C., Dumontet, B., Martí, E., Gorsky, G., Cózar, A., 2016. Changes in the floating plastic pollution of the Mediterranean sea in relation to the distance to land. PLoS One 11. https://doi.org/10.1371/journal.pone.0161581.

Pedrotti, M.L., Petit, S., Eyheraguibel, B., Kerros, M.E., Elineau, A., Ghiglione, J.F., Loret, J.F., Rostan, A., Gorsky, G., 2021. Pollution by anthropogenic microfibers in North-West Mediterranean Sea and efficiency of microfiber removal by a wastewater treatment plant. Sci. Total Environ. 758. https://doi.org/10.1016/j.scitotenv.2020.144195.

Persson, L., Carney Almroth, B.M., Collins, C.D., Cornell, S., de Wit, C.A., Diamond, M.L., Fantke, P., Hassellöv, M., MacLeod, M., Ryberg, M.W., Søgaard Jørgensen, P., Villarrubia-Gómez, P., Wang, Z., Hauschild, M.Z., 2022. Outside the safe operating space of the planetary boundary for novel entities. Environ. Sci. Technol. 56, 1510–1521. https://doi.org/10.1021/acs.est.1c04158.

Picheral, M., Irisson, O., 2017. EcoTaxa, a tool for the taxonomic classification of images. http://ecotaxa.obs-vlfr.fr (2017).

Plastics Europe, G.M.R, Conversio Market &amp, Strategy GmbH, 2019. Plastics - The Facts 2019. 14, p. 35.

Politikos, D.V., Ioakeimidis, C., Papatheodorou, G., 2017. Modeling the fate and distribution of floating litter particles in the Aegean Sea (E. Mediterranean). 4, pp. 1–18. https://doi.org/10.3389/fmars.2017.00191.

Reisser, J., Slat, B., Noble, K., Du Plessis, K., Epp, M., Proietti, M., De Sonneville, J., Becker, T., Pattiaratchi, C., 2015. The vertical distribution of buoyant plastics at sea: an observational study in the North Atlantic Gyre. Biogeosciences 12, 1249–1256. https://doi.org/10.5194/bg-12-1249-2015.

Rivers, M.L., Gwinnett, C., Woodall, L.C., 2019. Quantification is more than counting: actions required to accurately quantify and report isolated marine microplastics. Mar. Pollut. Bull. 139, 100–104. https://doi.org/10.1016/j.marpolbul.2018.12.024.

Ruiz-Orejón, L.F., Sardá, R., Ramis-Pujol, J., 2016. Floating plastic debris in the Central and Western Mediterranean Sea. Mar. Environ. Res. 120, 136–144. https://doi.org/10.1016/j.marenvres.2016.08.001.

Ryan, P.G., Moore, C.J., Van Franeker, J.A., Moloney, C.L., 2009. Monitoring the abundance of plastic debris in the marine environment. Philos. Trans. R. Soc. B Biol. Sci. 364, 1999–2012. https://doi.org/10.1098/rstb.2008.0207.

Scales, B.S., Cable, R.N., Duhaime, M.B., Gerdts, G., Fischer, F., Fischer, D., Mothes, S., Hintzki, L., Moldaenke, L., Ruwe, M., Kalinowski, J., Kreikemeyer, B., Pedrotti, M.L., Gorsky, G., Elineau, A., Labrenz, M., Oberbeckmann, S., 2021. Cross-hemisphere study reveals geographically ubiquitous, unexplored biosphere. Am. Soc. Microbiol. 6, 1–17.

Schmidt, N., Thibault, D., Galgani, F., Paluselli, A., Sempéré, R., 2018. Occurrence of microplastics in surface waters of the Gulf of Lion (NW Mediterranean Sea). Prog. Oceanogr. 163, 214–220. https://doi.org/10.1016/j.pocean.2017.11.010.

van Sebille, E., Wilcox, C., Lebreton, L., Maximenko, N., Hardesty, B.D., van Franeker, J.A., Eriksen, M., Siegel, D., Galgani, F., Law, K.L., 2015. A global inventory of small floating plastic debris. Environ. Res. Lett. 10, 124006. https://doi.org/10.1088/1748-9326/10/12/124006.

Ser-Giacomi, E., Baudena, A., Rossi, V., Follows, M., Clayton, S., Vasile, R., López, C., Hernández-García, E., 2021. Lagrangian betweenness as a measure of bottlenecks in dynamical systems with oceanographic examples. Nat. Commun. 12. https://doi.org/10.1038/s41467-021-25155-9.

Sorgente, R., Olita, A., Oddo, P., Fazioli, L., Ribotti, A., 2011. Numerical simulation and decomposition of kinetic energies in the Central Mediterranean Sea: insight on mesoscale circulation and energy conversion, pp. 1161–1214 https://doi.org/10.5194/osd-8-1161-2011.

Soto-Navarro, J., Jordá, G., Deudero, S., Alomar, C., Amores, Á., 2020. 3D hotspots of marine litter in the Mediterranean: a modeling study. Mar. Pollut. Bull. 155, 111159. https://doi.org/10.1016/j.marpolbul.2020.111159.

Spalding, M.D., Fox, H.E., Allen, G.R., Davidson, N., Ferdaña, Z.A., Finlayson, M., Halpern, B.S., Jorge, M.A., Lombana, A., Lourie, S.A., Martin, K.D., McManus, E., Molnar, J., Recchia, C.A., Robertson, J., 2007. Marine ecoregions of the world: a bioregionalization of coastal and shelf areas. Bioscience 57, 573–583. https://doi.org/10.1641/B570707.

Suaria, G., Avio, C.G., Mineo, A., Lattin, G.L., Magaldi, M.G., Belmonte, G., Moore, C.J., Regoli, F., Aliani, S., 2016. The Mediterranean plastic soup: synthetic polymers in Mediterranean surface waters. Sci. Rep. 6, 1–10. https://doi.org/10.1038/srep37551.

Ter Halle, A., Ladirat, L., Gendre, X., Goudouneche, D., Pusineri, C., Routaboul, C., Tenailleau, C., Duployer, B., Perez, E., 2016. Understanding the fragmentation pattern of marine plastic debris. Environ. Sci. Technol. 50, 5668–5675. https://doi.org/10.1021/acs.est.6b00594.

Trainic, M., Flores, J.M., Pinkas, I., Pedrotti, M.L., Lombard, F., Bourdin, G., Gorsky, G., Boss, E., Rudich, Y., Vardi, A., Koren, I., 2020. Airborne microplastic particles detected in the remote marine atmosphere. Commun. Earth Environ. 1, 1–9. https://doi.org/10.1038/s43247-020-00061-y.

UN/MAP, 2017. Mediterranean Quality Status Report. 539. Mediterr. Action Plan Barcelona Conv.

Van Melkebeke, M., Janssen, C., De Meester, S., 2020. Characteristics and sinking behavior of typical microplastics including the potential effect of biofouling: implications for remediation. Environ. Sci. Technol. 54, 8668–8680. https://doi.org/10.1021/acs.est.9b07378.

Weiss, L., Ludwig, W., Heussner, S., Canals, M., Ghiglione, J.F., Estournel, C., Constant, M., Kerhervé, P., 2021. The missing ocean plastic sink: gone with the rivers. Science (80-.) 373, 107–111. https://doi.org/10.1126/science.abe0290.

Zambianchi, E., Trani, M., Falco, P., 2017. Lagrangian transport of marine litter in the Mediterranean Sea. Front. Environ. Sci. 5, 1–15. https://doi.org/10.3389/fenvs.2017.00005.

Zayen, A., Sayadi, S., Chevalier, C., Boukthir, M., Ben, S., Tedetti, M., Bioproc, L., 2020. Microplastics in surface waters of the Gulf of Gabes, southern Mediterranean Sea: distribution, composition and influence of hydrodynamics. Estuar. Coast. Shelf Sci. 242, 106832. https://doi.org/10.1016/j.ecss.2020.106832.